

The Catalytic Effect in Opening an Organoactinide Metal Coordination Sphere: Regioselective Dimerization of Terminal Alkynes and Hydrosilylation of Alkynes and Alkenes with PhSiH₃ Promoted by Me₂SiCp''₂ThⁿBu₂

Aswini K. Dash, Ilya Gourevich, Ji Quan Wang, Jiaxi Wang, Moshe Kapon, and Moris S. Eisen*

Department of Chemistry and Institute of Catalysis Science and Technology, Technion–Israel Institute of Technology, Haifa 32000, Israel

Received June 7, 2001

This contribution describes the catalytic effect observed by opening the coordination sphere at an organoactinide complex. Replacing the pentamethylcyclopentadienyl ligand in Cp*₂-ThCl₂ (Cp* = C₅Me₅) by the bridge ligation [Me₂SiCp''₂]²⁻-2[Li]⁺ (Cp'' = C₅Me₄) affords the synthesis of *ansa*-Me₂SiCp''₂ThCl₂. The X-ray structure of this bridged complex coordinated to LiCl salt and solvent is presented, indicating the large coordinative unsaturation of the bridge organoactinides. This dichloro complex reacts with 2 equiv of BuLi, affording the corresponding dibutyl complex *ansa*-Me₂SiCp''₂Th(CH₂CH₂CH₂CH₃)₂, which was found to react extremely fast for the dimerization of terminal alkynes and also in the hydrosilylation of terminal alkynes or alkenes with PhSiH₃. Besides the rapidity of the processes using the bridge organoactinide, as compared to Cp*₂ThMe₂, the chemo- and regioselectivity of the products were *increased*, allowing the production of only the *gem*-dimer, the *trans*-vinylsilane, and the 1-silylated alkane for the dimerization, hydrosilylation of alkyne, and hydrosilylation of alkene processes, respectively. In the latter process, the corresponding alkane is always obtained as a byproduct. The rapidity of the processes is a consequence of the opening of the coordination sphere at the metal center, whereas the chemoselectivity and regioselectivity were achieved due to the hindered equatorial plane, attributed to the disposition of the methyl groups in the bridge ligation, forcing the incoming substrates to react with a specific regiochemistry. For the dimerization of alkynes the kinetic rate law is first order in organoactinide and exhibits two domains as a function of the alkyne concentration. At low alkyne concentrations, the reaction follows an inverse order, whereas at higher alkyne concentrations a zero order is observed. The turnover-limiting step is the carbon–carbon triple bond insertion of the terminal alkyne into the actinide acetylide bond to give the corresponding dimer. For the hydrosilylation of terminal alkyne or alkenes, the rate law for both processes follows a first order in catalyst and silane concentrations, although an inverse order is observed for either alkyne or alkene, respectively. D₂O quenching experiments between the organoactinide complex in the presence of 1-octene under starving PhSiH₃ conditions indicate the presence of a π-alkene complex responsible for the inverse order in all three processes. Plausible mechanistic scenarios are proposed.

Introduction

The stoichiometric and catalytic properties of organo-f-element complexes are deeply influenced by the nature of the π ancillary ligands.¹ Structurally, a considerable

opening of the metal coordination sphere (frontier orbitals)² at the σ-ligand equatorial girdle is obtained by replacing the pentamethylcyclopentadienyl ligation in Cp*₂MR₂ (Cp* = C₅Me₅, M = f-element metal, R = σ-bonded ligand) by a bridged ligation toward the corresponding *ansa*-Me₂SiCp''₂MR₂ (Cp'' = C₅Me₄).³ For organoactinides, this change allows an increase (10–100-fold) in rates for the olefin insertion into the M–R

(1) For general organoactinide and organoactinide reviews, see: (a) Edlmann, F. T.; Gun'ko, Y. K. *Coord. Chem. Rev.* **1997**, *165*, 163. (b) Ephritikhine, M. *New J. Chem.* **1992**, *16*, 451. (c) Edlmann, F. T. In *Comprehensive Organometallic Chemistry II*; Abel, E. W., Stone, F. G. A., Wilkinson, G., Eds.; Pergamon Press: Oxford, UK, 1995; Chapter 2, and references therein. (d) Stern, D.; Sabat, M.; Marks, T. J. *J. Am. Chem. Soc.* **1990**, *112*, 9558. (e) Anwander, R.; Herrman, W. A. *Top. Curr. Chem.* **1996**, *179*, 1. (f) Edlmann, F. T. *Top. Curr. Chem.* **1996**, *179*, 247. (g) Schumann, H.; Meese-Marktscheffel, J. A.; Esser, L. *Chem. Rev.* **1995**, *95*, 865. (h) Anwander, R. In *Applied Homogeneous Catalysis with Organometallic Compounds*; Cornils, B., Herrmann, W. A., Eds.; VCH Publishers: New York, 1996; Vol. 2, p 866. (i) Molander, G. A. *Chemtracs: Org. Chem.* **1998**, *11*, 237. (j) Ephritikhine, M. *New J. Chem.* **1992**, *16*, 451.

(2) (a) Bursten, B. E.; Strittmatter, R. J. *Angew. Chem., Int. Ed. Engl.* **1991**, *30*, 1069. (b) Tatsumi, K.; Nakamura, A. *J. Am. Chem. Soc.* **1987**, *109* (9), 3195.

(3) (a) Jeske, C.; Schock, L. E.; Mauermann, H.; Swepston, P. N.; Schumann, H.; Marks, T. J. *J. Am. Chem. Soc.* **1985**, *107*, 8103. (b) Jeske, C.; Lauke, H.; Mauermann, H.; Schumann, H.; Marks, T. J. *J. Am. Chem. Soc.* **1985**, *107*, 8111. (c) Fendrick, C. M.; Schertz, L. D.; Day, V. W.; Marks, T. J. *Organometallics* **1988**, *7*, 1828. (d) Fendrick, C. M.; Mintz, E. A.; Schertz, L. D.; Marks, T. J.; Day, V. W. *Organometallics* **1984**, *3*, 819.

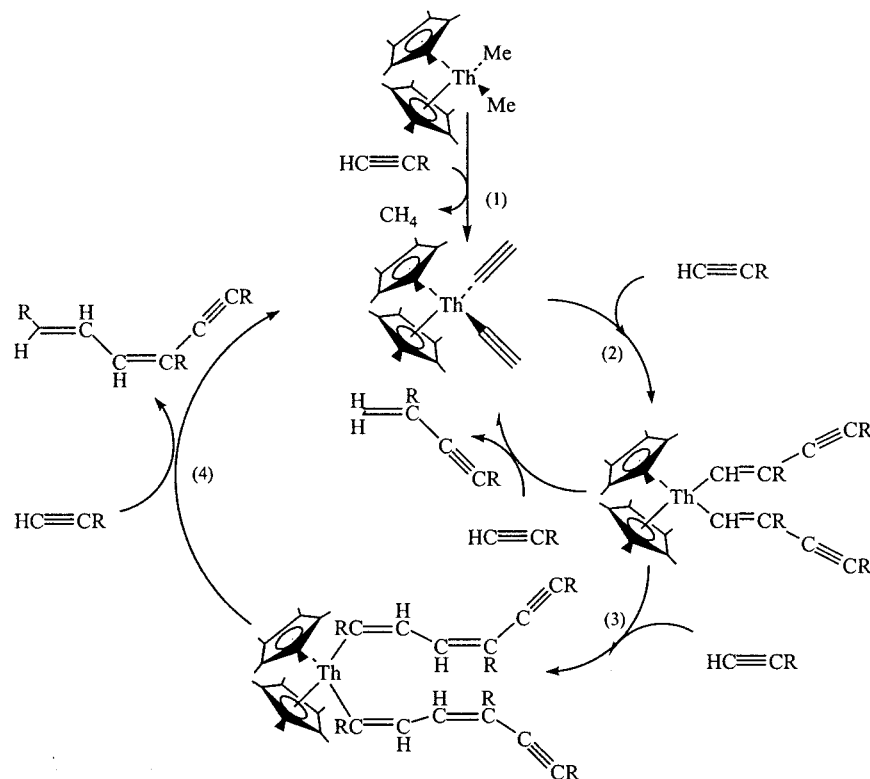


Figure 1. Proposed mechanistic pathway for the oligomerization of terminal alkynes promoted by $\text{Cp}^*_2\text{ThMe}_2$.

bond^{3a,b,4} and in organoactinides; this modification has been shown to cause an increase (10^3 -fold) in their catalytic activity for the hydrogenation of 1-hexene.^{3c,d} Recently, we have shown that organoactinides of the type Cp^*_2MR_2 ($\text{Cp}^* = \text{C}_5\text{Me}_5$; $\text{M} = \text{Th}, \text{U}$; $\text{R} = \text{CH}_3$) are active catalysts for either the oligomerization of terminal alkynes⁵ or the hydrosilylation of terminal alkynes with PhSiH_3 .⁶ In the former catalytic process the reaction was found to proceed with no regioselectivity, allowing the production of oligomers from dimers up to decamers. The lack in regioselectivity was observed due to the possible different modes of insertion of the terminal alkyne at the metal-carbyl bond at each growing step (steps 2 and 3 in Figure 1). The oligomerization kinetic rate law (eq 1) was measured, and the elimination of the alkenyl fragment from the organometallic moiety (step 4 in Figure 1) was found to be the rate-limiting step.

$$\nu = k[\text{alkyne}]^1[\text{Cp}^*_2\text{ThMe}_2]^1 \quad (1)$$

In the catalytic hydrosilylation process, the reaction was found to proceed rather slowly as compared to other lanthanide complexes,⁷ producing a myriad of hydrosilylated and hydrogenated products due to parallel competition processes. The kinetic rate law for the hydrosilylation of alkynes (eq 2) was shown to be operative with rapid alkyne insertion into a Th-H bond (step 1 in Figure 2), and the production of the hydrosi-

lated compound was found to be the rate-determining step (step 2 in Figure 2).

$$\nu = k[\text{alkyne}]^1[\text{PhSiH}_3]^1[\text{Cp}^*_2\text{ThMe}_2]^1 \quad (2)$$

In the rate-limiting step for both processes, the alkyne or silane approaches the corresponding metal-carbyl bond through the equatorial girdle between the two pentamethylcyclopentadienyl rings.⁸ Thus, a conceptual question arises regarding the use of an open organoactinide such as $\text{Me}_2\text{SiCp}''_2\text{Th}^n\text{Bu}_2$ as compared to $\text{Cp}^*_2\text{ThR}_2$. This opening in the coordination sphere at the metal center should increase the reactivity and at the same time the *selectivity* of the products in both oligomerization and hydrosilylation catalytic processes since any approach to the metal center through the equatorial plane is selectively hindered by the methyl groups of the bridged ancillary ligation.^{3,4} In this paper we report, and quantitatively compare, the effects of the *ansa*-

(7) For examples of catalytic activity of organolanthanides in hydrosilylation see: (a) Fu, P.-F.; Brard, L.; Li, Y.; Marks, T. J. *J. Am. Chem. Soc.* **1995**, *117*, 7157, and references therein. (b) Schumann, H.; Keitsch, M. R.; Winterfeld, J.; Muhle, S.; Molander, G. A. *J. Organomet. Chem.* **1998**, *559*, 181. (c) Sakakura, T.; Lautenschlager, H.; Tanaka, M. *J. Chem. Soc., Chem. Commun.* **1991**, 40. (d) Molander, G. A.; Dowdy, E. D.; Noll, B. C. *Organometallics* **1998**, *17*, 3754. (e) Onozawa, S.; Sakakura, T.; Tanaka, M. *Tetrahedron Lett.* **1994**, *35*, 8177. For complementary studies of group 4 metallocene-catalyzed hydrosilylation, see: (f) Takahashi, T.; Hasegawa, M.; Suzuki, N.; Saburi, M.; Rousset, C. J.; Fanwick, P. E.; Negishi, E. I. *J. Am. Chem. Soc.* **1991**, *113*, 8564. (g) Kesti, M. R.; Waymouth, R. M. *Organometallics* **1992**, *11*, 1095. (h) Kesti, M. R.; Abdulrahman, M.; Waymouth, R. M. *J. Organomet. Chem.* **1991**, *417*, C12. (i) Corey, J. Y.; Zhu, X. H. *Organometallics* **1992**, *11*, 672. (j) Harrod, J. F.; Yun, S. S. *Organometallics* **1987**, *6*, 1381. For group 3 complexes, see: (k) Molander, G. A.; Julius, M. *J. Org. Chem.* **1992**, *57*, 6347. (l) Molander, G. A.; Retsch, W. H. *Organometallics* **1995**, *14*, 4570.

(8) (a) Fagan, P. J. M., J. M.; Maatta, E. A.; Seyam, A. M.; Marks, T. J. *J. Am. Chem. Soc.* **1981**, *103*, 6650. (b) Elschenbroich, C.; Salzer, A. *Organometallics*, 1st ed.; VCH: Weinheim, Germany, 1989; Chapters 15 and 17.

(4) (a) Gagné, M. R.; Marks, T. J. *J. Am. Chem. Soc.* **1989**, *111*, 4108. (b) Giardello, M. A.; Conticello, V. P.; Brard, L.; Gagné, M. R.; Marks, T. J. *J. Am. Chem. Soc.* **1994**, *116*, 10241.

(5) (a) Haskel, A.; Straub, T.; Dash, A. K.; Eisen, M. S. *J. Am. Chem. Soc.* **1999**, *121*, 3014. (b) Haskel, A.; Wang, J. Q.; Straub, T.; Neyroud, T. G.; Eisen, M. S. *J. Am. Chem. Soc.* **1999**, *121*, 3025.

(6) Dash, A. K.; Wang, J. Q.; Eisen, M. S. *Organometallics* **1999**, *18*, 4724.

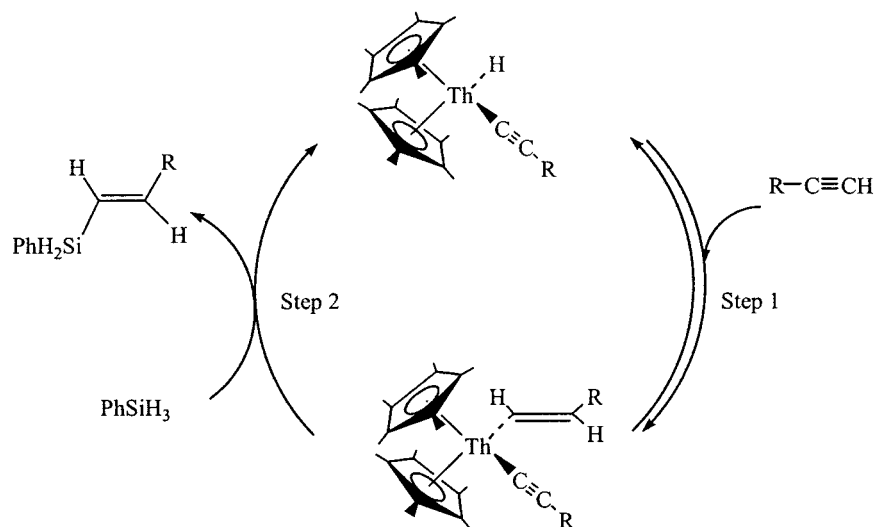


Figure 2. Proposed mechanistic pathway for the hydrosilylation of terminal alkynes with PhSiH_3 promoted by $\text{Cp}^*\text{-ThMe}_2$.

organothorium complex $\text{Me}_2\text{SiCp}^*\text{Th}^n\text{Bu}_2$ for the chemo- and regioselective dimerization of terminal alkynes as well as the rapid regioselective hydrosilylation of terminal alkynes and alkenes with PhSiH_3 . We present a kinetic and thermodynamic study for each one of the processes. In addition, a π -alkene–Th complex has been observed, indirectly linking the processes jointly and enabling the introduction of these findings in one comprehensive presentation to permit a good understanding for the kinetic results and offering an insight into the organoactinide-plausible mechanistic scenarios.

Experimental Section

Materials and Methods. All manipulations of air-sensitive materials were performed with the rigorous exclusion of oxygen and moisture in flamed Schlenk-type glassware on a dual manifold Schlenk line or interfaced to a high-vacuum (10^{-5} Torr) line or in a nitrogen-filled Vacuum Atmospheres glovebox with a medium capacity recirculator (1–2 ppm O_2). Argon and nitrogen were purified by passing them through a MnO oxygen-removal column and a Davison 4 Å molecular sieve column. Hydrocarbon solvents and benzene- d_6 were distilled under nitrogen from Na/K alloy. All solvents for vacuum line manipulations were stored in vacuo over Na/K alloy in resealable bulbs. $\text{Me}_2\text{SiCp}^*\text{Th}^n\text{Bu}_2$ was prepared according to the literature procedure.^{3c} Acetylenic and alkene compounds (Aldrich) were dried and stored over activated molecular sieves (4 Å), degassed, and freshly vacuum-distilled. Styrene was dried over CaO, distilled, and stored under vacuum. PhSiH_3 (Aldrich) was dried and stored over activated molecular sieves (4 Å), degassed, and freshly vacuum-distilled. D_2O and Ph_2SiH_2 (Aldrich) were used without further purifications. 1-Octene (dried over Na/K), *E*-2-octene, *E*-3-octene, and *E*-4-octene (Aldrich) were stored and dried over molecular sieves, 4 Å. NMR spectra were recorded on Bruker AM 200 and Bruker AM 400 spectrometers. ^1H NMR and ^{13}C NMR chemical shifts are referenced to internal solvent resonances and reported relative to tetramethylsilane. For ^{29}Si NMR, $\text{Si}(\text{TMS})_4$ was used as internal standard (Me_3Si at -7.80 ppm). GC/MS experiments were conducted in a GC/MS (Finnigan Magnum) spectrometer. The NMR experiments were conducted in Teflon valve-sealed tubes (J-Young) after vacuum transfer of the liquids in a high-vacuum line. The synthesis and characterization of *gem*- $\text{H}_2\text{C}=\text{C}(\text{Bu}^t)\text{C}=\text{C}(\text{Bu}^t)$ (**1**), *gem*- $\text{H}_2\text{C}=\text{C}(\text{Pr}^i)\text{C}=\text{C}(\text{Pr}^i)$ (**2**), *gem*- $\text{H}_2\text{C}=\text{C}(\text{Bu}^n)\text{C}=\text{C}(\text{Bu}^n)$ (**4**), *gem*- $\text{H}_2\text{C}=\text{C}(\text{Pr}^i)\text{C}(\text{H})=\text{C}(\text{Pr}^i)\text{C}\equiv\text{CPr}^i$ (**6**), *trans*- $\text{PrCH}=\text{CHSiH}_2\text{Ph}$

(**10**), *trans*- $^n\text{BuCH}=\text{CHSiH}_2\text{Ph}$ (**11**), *trans*- $\text{PhCH}=\text{CHSiH}_2\text{Ph}$ (**12**), *trans*- $p^t\text{Bu-PhCH}=\text{CHSiH}_2\text{Ph}$ (**13**), $^n\text{BuCH}_2\text{CH}_2\text{SiH}_2\text{Ph}$ (**19**), $\text{Ph}(\text{CH}_2)_2\text{SiH}_2\text{Ph}$ (**22**), and $\text{PhCH}(\text{CH}_3)\text{SiH}_2\text{Ph}$ (**23**) are described in the Supporting Information.

General Procedure for the Catalytic Dimerization of Terminal Alkynes. In a typical procedure, the specific amount of an alkyne was vacuum transferred in a high-vacuum line into a Schlenk flask containing the given amount of the precatalysts, $\text{Me}_2\text{SiCp}^*\text{Th}^n\text{Bu}_2$, in the denoted amount of the corresponding solvent. For $\text{MeC}\equiv\text{CH}$ and $^i\text{PrC}\equiv\text{CH}$ (low boiling point alkynes), a heavy glass Schlenk flask, suitable for high-pressure reactions, was used, and the reaction vessel was sealed by a J-Young stopcock. The Schlenk flask was heated by means of a thermostatic oil bath (± 0.1 °C), during a particular amount of time. The solvent was removed by vacuum, and the products were isolated through vacuum distillation (yields are reported). J-Young NMR tubes were filled in the glovebox. The percentage of the converted products is given related to the starting alkyne as measured by analytical GC chromatography and by NMR spectroscopy. In all the reactions, the volatiles and the residue were identified by ^1H , ^{13}C , and 2D (COSY, C–H correlation, NOESY) NMR spectroscopy, by GC/MS spectroscopy, and by comparing with compounds known in the literature.

(1) Dimerization of Olefin-Functionalized Substituted Terminal Alkynes. (a) The reaction of 15.7 mL (165 mmol) of $\text{H}_2\text{C}=\text{C}(\text{Me})\text{C}\equiv\text{CH}$ with 50 mg of $\text{Me}_2\text{SiCp}^*\text{Th}^n\text{Bu}_2$ (7.76×10^{-2} mmol) in 50 mL of C_6H_6 , at room temperature, produced the corresponding head-to-head dimer, *gem*- $\text{H}_2\text{C}=\text{C}(\text{Me})=\text{CH}_2\text{C}\equiv\text{C}(\text{Me})=\text{CH}_2$ (**3**) with yields of 46% or 78% after 16 and 45 h, respectively. When the reaction mixture was allowed to stir longer at room temperature, a new set of signals slowly appeared in the olefinic region in the ^1H NMR for the protons of the intermolecular Diels–Alder adduct **8** with concurrent reduction in the intensity of the signals corresponding to *gem*- $\text{H}_2\text{C}=\text{C}(\text{Me})=\text{CH}_2\text{C}\equiv\text{C}(\text{Me})=\text{CH}_2$ (**3**). After 7 days of stirring at room temperature a 45% yield of the intermolecular Diels–Alder adduct **8** was obtained (maximum yield is 50%), and 10% yield of the *gem*- $\text{H}_2\text{C}=\text{C}(\text{Me})=\text{CH}_2\text{C}\equiv\text{C}(\text{Me})=\text{CH}_2$ (**3**) was left in the reaction mixture.

(b) The reaction of 15.7 mL (165 mmol) of $\text{H}_2\text{C}=\text{C}(\text{Me})\text{C}\equiv\text{CH}$ with 50 mg of $\text{Me}_2\text{SiCp}^*\text{Th}^n\text{Bu}_2$ (7.76×10^{-2} mmol) in 50 mL of C_6H_6 at 78 °C for 2 h produced the *gem*- $\text{H}_2\text{C}=\text{C}(\text{Me})=\text{CH}_2\text{C}\equiv\text{C}(\text{Me})=\text{CH}_2$ dimer (**3**; 33%) and the intermolecular Diels–Alder adduct **8** (34%) with a conversion of 70% with respect to alkyne. A complete conversion into the Diels–Alder adduct (49%) was observed after 6 h refluxing compound **3**, under similar reaction conditions. The Diels–Alder adduct was

also prepared independently by heating compound **3** without the organoactinide catalyst in C₆H₆ at 78 °C for 5 h. Compound **8** was purified through a silica gel column eluted with CH₂-Cl₂. Removal of the solvent by flash evaporation gave compound **8** in 97% yield.

Spectroscopy data for *gem*-H₂C=C(C(Me)=CH₂)C≡C-C(Me)=CH₂ (3**).** Bp = 50–55 °C at 5 mmHg. ¹H NMR (C₆D₆, 200 MHz): δ 5.52 (s, 1H, HCH), 5.27 (s, 1H, HCH), 5.84 (s, 1H, HCH), 5.07 (s, 1H, HCH), 5.34 (s, 1H, HCH), 5.02 (s, 1H, HCH), 1.75 (s, 3H, CH₃), 1.69 (s, 3H, CH₃). ¹³C NMR (C₆D₆, 50 MHz): δ 140.9 (s, 2 C(Me)=CH₂), 132.5 (s, C=CH₂), 121.8 (s, CH₂), 120.8 (s, CH₂), 117.32 (s, CH₂), 92.2 (s, C≡C), 87.6 (s, C∞C), 23.37 (s, CH₃), 19.26 (s, CH₃). GC/MS: *m/z* 132 (M⁺), 117 (M⁺ - CH₃, 100%), 103 (M⁺ - C₂H₅), 91 (M⁺ - C₃H₅), 77 (M⁺ - C₄H₇), 63 (M⁺ - C₅H₇). HRMS (*m/z*): {M⁺} calcd for C₁₀H₁₂ = 132.0939, found 132.0924. Anal. Calcd for C₁₀H₁₂: C, 90.85; H, 9.15. Found: C, 90.39; H, 9.37.

Spectroscopic Data for Intermolecular Diels–Alder Adduct **8.** ¹H NMR (C₆D₆, 200 MHz): δ 5.35 (s, 1H, HCH), 5.25 (s, 1H, HCH), 5.04 (s, 1H, HCH), 4.96 (s, 1H, HCH), 4.94 (s, 1H, HCH), 4.82 (s, 1H, HCH), 2.68 (m, 2H, CH₂), 2.27 (bs, 1H, HCH), 2.19 (bs, 1H, HCH), 1.92 (s, 3H, CH₃), 1.85 (s, 3H, CH₃), 1.81 (s, 3H, CH₃), 1.71 (s, 3H, CH₃), 1.56 (m, 2H, CH₂). ¹³C NMR (C₆D₆, 50 MHz): δ 147.6 (s, 2 C(Me)=CH₂), 138.6 (s, sp²C), 121.8 (s, sp²C), 120.8 (s, =CH₂), 120.4 (s, =CH₂), 114.5 (s, sp²C), 110.6 (s, =CH₂), 93.7 (C≡C), 93.0, (C≡C), 89.7 (s, C≡C), 83.9 (s, C≡C), 42.5 (s, CH₂), 32.9 (s, sp³C) 31.9 (s, CH₂), 28.4 (s, CH₂), 23.8 (s, 2 CH₃), 22.1 (s, CH₃), 19.6 (s, CH₃). GC/MS: *m/z* 264 (M⁺), 263 (M⁺ - H), 249 (M⁺ - CH₃), 236 (M⁺ - 2CH₃), 221 (M⁺ - 3CH₃), 207 (M⁺ - 3Me - CH₂), 193 (M⁺ - 3Me - 2CH₂), 179 (M⁺ - 3Me - 3CH₂), 91 (H₂C=C(Me)-C(=CH₂)C≡C⁺), 77 (91 - CH₂), 65 (H₂C=C(Me)C≡C⁺), 53 (H₂C=C(Me)C⁺). HRMS (*m/z*): {M⁺} calcd for C₂₀H₂₄ 264.1878, found 264.1872. Anal. Calcd for C₂₀H₂₄: C, 90.85; H, 9.15. Found: C, 90.54; H, 9.31.

(2) Dimerization of MeC≡CH. The reaction of 360 mg (*d* = 0.6911 g/cm³ at -40 °C) (1.0 mmol) of MeC≡CH (measured at low temperature, -40 °C, when the alkyne is liquid) with 50 mg of Me₂SiCp^{''}₂Th^{''}Bu₂ (7.76 × 10⁻² mmol) in C₆H₆ at room temperature for 48 h (careful-pressure Schlenk flasks with pressure valves should be used) produced the *gem*-H₂C=C(Me)C≡C(Me) (**5**) in 70% conversion. The remaining 30% was the starting material. Slow release of the pressure in a well-ventilated hood and distillation of the dimer allows the production of the clean dimer **5** in 64% yield.

Spectroscopic Data for *gem*-H₂C=C(Me)C≡C(Me) (5**).** Bp = 83–86 °C at 760 mmHg. ¹H NMR (C₆D₆, 200 MHz): δ 5.29 (s, 1H, HCH), 5.01 (s, 1H, HCH), 1.77 (s, 3H, CH₃), 1.57 (s, 3H, CH₃). ¹³C NMR (C₆D₆, 50 MHz): δ 134.2 (s, C=CH₂), 120.2 (t, *J* = 159 Hz, CH₂), 90.5 (s, C≡CMe), 85.1 (s, C≡CMe), 3.7 (q, *J* = 131 Hz, CH₃), 2.7 (q, *J* = 131 Hz, CH₃). HRMS (*m/z*): {M⁺} calcd for C₆H₈ 80.1277, found 80.1269. Anal. Calcd for C₆H₈: C, 89.94; H, 10.06. Found: C, 89.67; H, 10.22.

Kinetic Study for the Dimerization of **2.** In a typical experiment an NMR sample was prepared by reacting the specific amount of alkyne and the corresponding organoactinide into a J-Young NMR tube containing the particular amount of the corresponding solvent. The sealed tube was maintained at -78 °C until kinetic measurements were initiated. The sealed tube was heated in a temperature-controlled oil bath, and at time intervals NMR data were acquired using eight scans per time interval with a long pulse delay to avoid saturation of the signal. The conversion was measured by following the intensity of the acetylenic hydrogen of the alkyne. The kinetic studies were usually monitored by the intensity changes in both the substrate resonances and in the product resonances over 3 or more half-lives. The substrate concentration (*C*) was measured from the area (*A_s*) of the ¹H-normalized signal of the solvent (*A_b*). All the data collected could convincingly fit (*R* > 0.98) by least-squares to eq 3 or 4 where *C*₀ (*C*₀ = *A_{so}*/*A_{bo}*) is the initial concentration of substrate,

and *C* (*A_s*/*A_b*) is the substrate concentration at time, *t*.

$$mt = \log(C/C_0) \quad (3)$$

$$\frac{1}{C} = \frac{1}{C_0} + mt \quad (4)$$

The ratio of catalyst to substrate was accurately measured by calibration with internal FeCp₂. Turnover frequencies (*N_t*, h⁻¹) were calculated from the least-squares determined slopes (*m*) of the resulting plots. Typical initial alkyne concentrations were in the range 0.25–6.22 M, and typical catalyst concentrations were in the range 2.1–25 mM.

General Procedure for the Catalytic Hydrosilylation of Terminal Alkynes. In a typical procedure, the specific alkyne and an equimolar amount of PhSiH₃ were vacuum transferred in a high-vacuum line into a Schlenk flask containing 50 mg of Me₂SiCp^{''}₂Th^{''}Bu₂ (7.76 × 10⁻² mmol) in 25 mL of C₆H₆. A gastight syringe transferred aliquot amounts of the reaction mixture into a GC chromatograph or into a J-Young NMR tube. The NMR tube was then connected to a vacuum line where the benzene was evaporated and deuterated benzene was refilled. The sealed flask was maintained at room temperature until 100% conversion of the alkyne was detected by either the disappearance of the alkyne in the GC or the disappearance of the acetylenic hydrogen of the alkyne by ¹H NMR spectroscopy. The percentage of the converted products is given related to the alkyne. The organic products were either distilled under vacuum or cleaned by passing them through a short silica gel column (Merck 60 Å) eluted with hexane. All products were identified by ¹H, ¹³C, ²⁹Si, and 2D NMR spectroscopy, GC/MS spectroscopy, and microanalysis and by comparing with literature known compounds.

(3) Hydrosilylation of ^tBuC≡CH with PhSiH₃. The reaction of 1.76 mL (14.3 mmol) of ^tBuC≡CH with 1.76 mL (14.3 mmol) of PhSiH₃ catalyzed by 50 mg of Me₂SiCp^{''}₂Th^{''}Bu₂ (7.76 × 10⁻² mmol) in 25 mL of C₆H₆ produced the regioselective hydrosilylation product, *trans*-^tBuCH=CHSiH₂Ph (**9**), in 95% conversion (90% yield) after 15 min at room temperature. The reaction mixture was allowed to stir for an additional 30 min, leading to 100% conversion (98% yield) into **9**. The solvent was removed by flash evaporation, and the product was distilled, collecting the fraction at 78–86 °C at 0.5 mmHg. ¹H NMR (200 MHz, C₆D₆): δ 7.05–7.17 (m, 3H, *o-p-H*Ph), 7.60–7.64 (m, 2H, *m-H*Ph), 6.39 (d, 1H, ³*J*_{trans} = 18.8 Hz, HCBu^o), 5.62 (dt, 1H, ³*J*_{trans} = 18.8 Hz, ³*J*_{H(Si)} = 3.2 Hz, HC(PhSiH₂)), 4.79 (d, 2H, ³*J* = 3.2 Hz, PhSiH₂), 0.90 (s, 9H, C(CH₃)₃). ¹³C NMR (50 MHz, C₆D₆): δ 164.1 (d, ¹*J* = 152 Hz, HCBu^o), 135.6, 129.8, 128.3 (C-H-Ph), 132.5 (s, CC₅H₅), 114.2 (d, ¹*J* = 141 Hz, HC(PhSiH₂)), 32.2 (s, CMe₃), 28.8 (q, ¹*J* = 128 Hz, C(CH₃)₃). ²⁹Si NMR (79.5 Hz, C₆D₆): δ 15.62 (tt, ¹*J*_{Si-H} = 198 Hz, ³*J*_{Si-H} = 7.3 Hz, PhSiH₂). GC/MS data: *m/z* 190 (M⁺), 189 (M⁺ - H), 175 (M⁺ - CH₃), 162 (M⁺ - C₂H₄), 148 (M⁺ - C(CH₃)₂), 133 (M⁺ - C(CH₃)₃), 120 (M⁺ - (CH₃)₃-CCH), 105 (PhSi⁺, 100%). HRMS (*m/z*): {M⁺} calcd for C₁₂H₁₈-Si 190.1178, found 190.1171. Anal. Calcd for C₁₈H₁₈Si: C, 75.71; H, 9.53. Found: C, 75.45; H, 9.39.

(4) Hydrosilylation of HC≡C-C(Me)=CH₂ with PhSiH₃. According to the general procedure described above, the reaction of 9.8 mL (10.0 mmol) of HC≡C-C(Me)=CH₂ with 12.8 mL (10.0 mmol) of PhSiH₃ catalyzed by 50 mg of Me₂-SiCp^{''}₂Th^{''}Bu₂ (7.76 × 10⁻² mmol) in 10 mL of C₆H₆ at room temperature produced the regioselective hydrosilylation product *trans*-H₂C=C(Me)CH=CHSiH₂Ph (**14**) in 72% yield after 15 min at room temperature. When the reaction mixture was allowed to stir for 60 min, 100% conversion into **14** was obtained. Distillation of the product allows the isolation of 95% yield. Addition of another 10.0 mmol of PhSiH₃ to the reaction mixture does not induce the hydrosilylation of any of the olefin moieties in **14**, neither at room nor at reflux temperature.

Spectroscopic Data for *trans*-H₂C=C(Me)CH=CHSiH₂Ph (14). Bp of **14** = 65–75 at 0.3 mmHg. ¹H NMR (200 MHz, C₆D₆): δ 7.49–7.54 (m, 2H, *m*-H-Ph), 7.13–7.16 (m, 3H, *o*, *p*-H-Ph), 6.89 (d, ³J_{trans} = 18.68 Hz, 1H, CH(C(Me)=CH₂)), 5.77 (dt, ³J_{trans} = 18.7 Hz, ³J_{HH(Si)}} = 3.23 Hz, 1H, CHSiH₂Ph), 4.95 (s, 1H, HCH), 4.91 (s, 1H, HCH), 4.79 (d, *J* = 3.25 Hz, 2H, SiH₂Ph), 1.66 (s, 3H, CH₃). ¹³C NMR (50 MHz, C₆D₆): δ 152.5 (s, CH(C(Me)=CH₂)), 143.3 (s, C(Me)=CH₂), 135.8, 130.1, 128.5 (C-H-Ph), 132.0 (s, CC₅H₅), 119.6 (s, CHSiH₂Ph), 119.0 (s, H₂C=), 17.8 (s, CH₃). ²⁹Si NMR (79.5 MHz, C₆D₆): δ 15.1 (t, *J* = 198.6 Hz, PhSiH₂). LRMS (EI) *m/z* 174 (M⁺), 159 (M⁺ - CH₃), 145 (M⁺ - C₂H₅), 131 (M⁺ - C₃H₇), 105 (PhSi⁺, 100%). HRMS calcd for C₁₁H₁₄Si 174.0865, found 174.0864. Anal. Calcd for C₁₁H₁₄Si: C, 75.79; H, 8.10. Found: C, 75.38; H, 8.03.

(5) Metathesis Reactions of *trans*-PrCH=CHSiH₂Ph with RC≡CH (R = ⁱPr, ^tBu). (a) Compound **10** was obtained in >99% conversion (92% yield) by the reaction of 1.38 mL (13.5 mmol) of ⁱPrC≡CH with 1.67 mL (13.5 mmol) of PhSiH₃ catalyzed by 50 mg of Me₂SiCp[∗]₂Th[∗]Bu₂ (7.76 × 10⁻² mmol) in 15 mL of C₆H₆, at room temperature after 60 min. Then 1.38 mL (13.5 mmol) of ⁱPrC≡CH was transferred by vacuum transfer (after being measured in a small J-Young calibrated vessel) into the reaction mixture, and the solution was allowed to stir at room temperature for 78 h, producing *trans*-PrCH=CHSi(H)(Ph)C≡CPrⁱ (**15**; 60%) and ⁱPrCH=CH₂ (**16**; 35%). A 56% conversion was observed with respect to *trans*-PrCH=CHSiH₂Ph (**10**). Flash evaporation of the reaction mixture allows the elimination of the alkene (recognized by GC retention time), and passing the residual reaction mixture through a 10 cm length silica gel column, eluted with hexane, allows the purification of **15** as a pale yellow oil in 52% yield.

Spectroscopic Data for *trans*-PrCH=CHSi(H)(Ph)C≡CPrⁱ (15). ¹H NMR (200 MHz, C₆D₆): δ 7.74–7.81 (m, 2H, *m*-H-Ph), 7.21–7.30 (m, 3H, *o*, *p*-H-Ph), 6.51 (dd, ³J_{trans} = 18.43 Hz, ³J_{HH(Pr)}} = 5.86 Hz, 1H, HCPrⁱ), 5.75 (dd, ³J_{trans} = 18.43 Hz, ³J_{HH(Si)}} = 2.77 Hz, 1H, HCSiHPh), 5.15 (d, *J* = 2.77 Hz, 1H, SiHPh), 2.40 (m, 1H, CHPrⁱ), 2.18 (septet, *J* = 6.95 Hz, 1H, CHPrⁱ), 1.02 (d, *J* = 6.74 Hz, 6H, CH(CH₃)₂), 0.85 (d, *J* = 6.95 Hz, 6H, CH(CH₃)₂). ¹³C NMR (50 MHz, C₆D₆): δ 159.6 (s, CHPrⁱ), 135.2, 129.9, 128.3 (s, CH-Ph), 132.4 (s, CC₅H₅), 118.9 (s, CHSiHPh), 117.1 (s, C≡C), 77.5 (s, C≡C), 34.6 (s, CHMe₂), 34.8 (s, CHMe₂), 22.8 (s, CH(CH₃)₂), 21.6 (s, CH(CH₃)₂). ²⁹Si NMR (79.5 MHz, C₆D₆): δ 8.5 (d, *J* = 210 Hz, PhSiH). GC/MS: *m/z* 242 (M⁺), 241 (M⁺ - H), 227 (M⁺ - CH₃), 214 (M⁺ - C₂H₄), 199 (M⁺ - Prⁱ), 186 (M⁺ - ⁱPr - CH), 173 (M⁺ - ⁱPrCH=CH) 157 (M⁺ - ⁱPr - C₃H₆), 145 (M⁺ - C₇H₁₃), 131 (PhSiH₂C≡C⁺), 105 (PhSi⁺, 100%). HRMS calcd for C₁₆H₂₂Si 242.1491, found 242.1486. Anal. Calcd for C₁₆H₂₂Si: C, 79.27; H, 9.15. Found: C, 79.66; H, 9.31.

(b) A 1.66 mL sample of ^tBuC≡CH (13.5 mmol) was vacuum transferred (after being measured) into a Schlenk tube containing compound **10** as prepared in part (a), and the solution was allowed to stir at room temperature for 78 h, producing *trans*-PrCH=CHSi(H)(Ph)C≡CBu^t (**17**; 63%) and ^tBuCH=CH₂ (**18**; 33%). A 50% conversion was observed with respect to *trans*-PrCH=CHSiH₂Ph (**2**). Flash distillation on the reaction mixture allows the elimination of the alkene, and passing the mixture through a 10 cm length silica gel column, eluted with hexane, allows the purification of **17** as a pale yellow oil in 54%.

Spectroscopic Data for *trans*-PrCH=CHSi(H)(Ph)C≡CBu^t (17). ¹H NMR (200 MHz, C₆D₆): δ 7.76–7.82 (m, 2H, *m*-H-Ph), 7.08–7.23 (m, 3H, *o*, *p*-H-Ph), 6.49 (dd, ³J_{trans} = 18.4 Hz, ³J_{HH(Pr)}} = 5.87 Hz, 1H, HCPr^t), 5.73 (dd, ³J_{trans} = 18.4 Hz, ³J_{HH(Si)}} = 2.48 Hz, 1H, HCSiHPh), 5.17 (d, *J* = 2.94 Hz, 1H, SiHPh), 2.15 (m, 1H, CHPr^t), 1.14 (s, 9H, C(CH₃)₃), 0.86 (d, *J* = 6.73 Hz, 6H, CH(CH₃)₂). ¹³C NMR (50 MHz, C₆D₆): δ 159.7 (s, CHPr^t), 135.5, 129.9, 128.3 (s, CH-Ph), 132.5 (s, CC₅H₅), 119.0 (s, CHSiHPh), 114.2 (s, C≡C), 76.6 (s, C≡C), 34.5 (s, CHMe₂), 30.8 (s, CMe₃), 30.6 (s, C(CH₃)₃), 21.5 (s, CH(CH₃)₂). ²⁹Si NMR (79.5 MHz, C₆D₆): δ 8.6 (d, *J* = 211 Hz, PhSiH).

GC/MS: *m/z* 256 (M⁺), 255 (M⁺ - H), 241 (M⁺ - CH₃), 228 (M⁺ - C₂H₆), 213 (M⁺ - Pr^t), 200 (M⁺ - C₄H₈), 199 (M⁺ - Bu^t), 187 (BuC≡CSiHPh⁺), 159 (187 - C₂H₆), 145 (187 - C₃H₆), 129 (187 - Bu^t - H), 105 (PhSi⁺, 100%). HRMS calcd for C₁₇H₂₄Si 256.1647, found 256.1635. Anal. Calcd for C₁₇H₂₄Si: C, 79.62; H, 9.43. Found: C, 79.43; H, 9.28.

General Procedure for the Catalytic Hydrosilylation of Alkenes. In a typical procedure the specific alkene and an equimolar amount of PhSiH₃ were vacuum transferred in a high-vacuum line into a Schlenk flask containing either 50 mg of Me₂SiCp[∗]₂Th[∗]Bu₂ (7.76 × 10⁻² mmol) or 100 mg of Cp[∗]₂ThMe₂ (0.187 mmol) in the indicated amount of C₆H₆. A gastight syringe transferred aliquot amounts of the reaction mixture into a GC chromatograph or into a J-Young NMR tube. The NMR tube was then connected to a vacuum line, where the benzene was evaporated and deuterated benzene was filled. The sealed flask was maintained at room temperature until 100% conversion of the alkene was detected by either the disappearance of the vinylic hydrogen of the alkene by ¹H NMR spectroscopy or the disappearance of the alkene in the GC. The percentage of the converted products is given relative to the alkene. The organic products were either distilled under vacuum or cleaned by passing them through a short silica gel column (Merck 60 Å) eluting with hexane. All products were identified by ¹H, ¹³C, ²⁹Si, and 2D-NMR spectroscopy, GC-MS spectroscopy, and microanalysis and by comparing with known literature compounds. In all the alkene hydrosilylation reactions catalyzed by Cp[∗]₂ThMe₂, equimolar amounts of PhSiH₂Me, trace amounts of Ph₂SiH₂, and trace amounts of the products corresponding to the dehydrogenative coupling of silanes from the dimer PhH₂SiSiH₂Ph to higher oligomers were observed either by GC-MS or by the ²⁹Si NMR of the reaction mixtures. When the reactions are catalyzed by Me₂SiCp[∗]₂Th[∗]Bu₂, the same byproducts are always obtained as with Cp[∗]₂ThMe₂, although instead of PhSiH₂Me, equimolar amounts of the corresponding PhSiH₂Bu are obtained.

(6) Hydrosilylation of 1-Octene with PhSiH₃ Catalyzed by Cp[∗]₂ThMe₂ and Me₂SiCp[∗]₂Th[∗]Bu₂. (a) The reaction of 1.0 mL (6.26 mmol) of 1-octene with 0.80 mL (6.40 mmol) of PhSiH₃ catalyzed by 100 mg of Cp[∗]₂ThMe₂ (0.187 mmol) in 15 mL of C₆H₆ at room temperature produces quantitative conversion of the alkene (>98%) to yield the hydrosilylation product CH₃(CH₂)₆CH₂SiH₂Ph (**20**) in 68% and the hydrogenation product *n*-octane in 30% conversion after 12 h. Flash evaporation of the octane at 127 °C and distillation of the silane under vacuum allows the separation of **20** in 62% yield.

(b) As described in (a), >98% conversion was obtained from the reaction of 1.0 mL (6.26 mmol) of 1-octene with 0.80 mL (6.40 mmol) of PhSiH₃ catalyzed by 50 mg of Me₂SiCp[∗]₂Th[∗]Bu₂ (7.6 × 10⁻² mmol) in 15 mL of C₆H₆ at room temperature. The hydrosilylation product CH₃(CH₂)₆CH₂SiH₂Ph was obtained in 65% and the hydrogenation product *n*-hexane in 33% after 12 h. Separation of the silane was performed as described in part (a). Bp of **20** = 158–163 °C at 20 mmHg. ¹H NMR (200 MHz, C₆D₆) δ 7.48–7.44 (m, 2H, *m*-H-Ph), 7.17–7.14 (m, 2H + 1H, *o*, and *p*-H-Ph), 4.43 (t, ³J_{HH} = 3.6 Hz, 2H, SiH₂Ph), 1.41–1.10 (m, 12H, CH₃(CH₂)₆CH₂SiH₂Ph), 0.91–0.78 (m, 5H, CH₃(CH₂)₆CH₂SiH₂Ph). ¹³C NMR (50 MHz, THF-*d*₆): δ 135.4 (Ph), 132.8 (Ph), 129.6 (Ph), 128.2 (Ph), 33.2, 32.3, 29.6, 25.5, 23.0, 22.1 (CH₂), 14.3 (CH₃), 10.4 (CH₂Si). ²⁹Si NMR (79.5 MHz, C₆D₆): δ 21.15 (t, *J* = 192.8 Hz, PhSiH₂). GC/MS data: *m/z* 220 (M⁺), 219 (M⁺ - H), 163 (M⁺ - C₄H₉), 143 (M⁺ - C₆H₅), 135 (M⁺ - C₆H₁₃), 121 (M⁺ - C₇H₁₅), 107 (PhSiH₂⁺ - 100%), 85 (C₆H₁₃⁺). HRMS calcd for C₁₄H₂₄Si 220.4259; found 220.4232. Anal. Calcd for C₁₄H₂₄Si: C, 76.28; H, 10.97. Found: C, 76.51; H, 10.60.

(7) Hydrosilylation of Allyl Benzene with PhSiH₃ Catalyzed by Cp[∗]₂ThMe₂ and Me₂SiCp[∗]₂Th[∗]Bu₂. (a) Quantitative conversion (>98%) of the alkene was obtained by the reaction of 1.20 mL (8.90 mmol) of allylbenzene with 1.10 mL (8.90 mmol) of PhSiH₃ catalyzed by 100 mg of Cp[∗]₂ThMe₂

(0.187 mmol) in 15 mL of C₆H₆ at 78 °C for 6 h. The reaction mixture contains 61% of the hydrosilylated allyl benzene Ph(CH₂)₃SiH₂Ph (**21**) and 38% of propylbenzene. Flash evaporation of the propylbenzene at 159 °C and distillation of the silane under vacuum (bp = 100–102 °C at 0.04 mmHg) allows the separation of **21** in 53% yield.

(b) According to the general hydrosilylation procedure described above, >98% conversion was obtained in 1 h at 78 °C from the reaction of 1.20 mL (8.90 mmol) of allylbenzene with 1.10 mL (8.90 mmol) of PhSiH₃ catalyzed by 50 mg of Me₂SiCp*₂ThⁿBu₂ (7.6 × 10⁻² mmol) in 15 mL of C₆H₆. The hydrosilylation product Ph(CH₂)₃SiH₂Ph (**21**) was obtained in 71% and the hydrogenation product propylbenzene was obtained in 29% yield. Separation of the silane was performed as described in part (a). Bp of **21** = 100–102 °C at 0.04 mmHg. ¹H NMR (200 MHz, C₆D₆): δ 7.46–7.41 (m, 4H, *m-H*-Ph), 7.16–6.96 (m, 6H *o*, and *p-H*-Ph), 4.44 (t, ³J_{HH} = 3.7 Hz, 2H, SiH₂Ph), 2.46 (t, ³J_{HH} = 7.6 Hz, 2H, PhCH₂), 1.64 (q, ³J_{HH} = 7.6 Hz, 2H, PhCH₂CH₂CH₂), 0.83–0.71 (m, 2H, CH₂SiH₂Ph). ¹³C NMR (50 MHz, C₆D₆): δ 144.6 (C_{ipso}), 137.8 (Ph), 134.4 (C_{ipso}), 131.9 (C_{para}), 128.6 (Ph), 128.4 (Ph), 127.8 (Ph), 126.1 (C_{para}), 39.2 (PhCH₂), 27.3 (PhCH₂CH₂), 10.0 (CH₂SiH₂Ph). ²⁹Si NMR (79.5 MHz, C₆D₆): δ 21.17 (t, *J* = 193.1 Hz, PhSiH₂). GC/MS data: *m/z* 226 (M⁺), 225 (M⁺ – H), 148 (M⁺ – C₆H₆), 135 (M⁺ – C₇H₉), 121 (M⁺ – C₈H₁₃), 107 (PhSiH₂⁺ – 100%), 91 (C₇H₇⁺). HRMS calcd for C₁₅H₁₈Si 226.1178; found 226.1175. Anal. Calcd for C₁₅H₁₈Si: C, 79.58; H, 8.01. Found: C, 79.34; H, 7.90.

Kinetic Study of the Hydrosilylation Reactions. In a typical experiment, an NMR sample was prepared by reacting the specific amounts of alkyne or alkene with a specific amount of the PhSiH₃ and the corresponding amount of the organoactinide into a J-Young NMR tube containing the particular amount of the corresponding solvent. The sealed tube was maintained at –78 °C until kinetic measurements were initiated. The sealed tube was heated in a temperature-controlled NMR spectrometer, and the data were acquired using eight scans per time interval with a long pulse delay to avoid saturation of the signal. The conversion was measured by following the intensity of the acetylenic hydrogen of the alkyne or the vinylic hydrogen of the alkene. The kinetic studies were usually monitored by the intensity changes in both the substrate resonances and in the product resonances over 3 or more half-lives. The substrate concentration (*C*) was measured from the area (*A_s*) of the ¹H-normalized signal of the solvent (*A_b*). All the data collected could convincingly fit (*R* > 0.98) by least-squares to eq 3 or 4, where *C*₀ (*C*₀ = *A_{so}*/*A_{bo}*) is the initial concentration of substrate, and *C*(*A_s*/*A_b*) is the substrate concentration at time, *t*.

$$mt = \log(C/C_0) \quad (3)$$

$$\frac{1}{C} = \frac{1}{C_0} + mt \quad (4)$$

The ratio of catalyst to substrate was accurately measured by calibration with internal FeCp₂. Turnover frequencies (*N_t*, h⁻¹) were calculated from the least-squares-determined slopes (*m*) of the resulting plots. For the hydrosilylation of alkynes, typical initial alkyne concentrations were in the range 0.10–4.18 M, initial silane concentrations were in the range 0.40–4.30 M, and typical catalyst concentrations were in the range 3.0–40.0 mM. For the hydrosilylation of alkenes, typical initial alkene concentrations were in the range 0.341–3.410 M, initial silane concentrations were in the range 0.176–1.760 M, and typical catalyst concentrations were in the range 6.30–84.60 mM.

(8) Isomerization Reaction of 1-Octene. In a typical experiment a Schlenk flask was charged in the glovebox with 20 mg (0.0375 mmol) of Cp*₂ThMe₂. A 0.3 mL sample of 1-octene and 5 mL of benzene were vacuum transferred to the

Table 1. Crystal Data and Structure Refinement for the Complex Me₂SiCp*₂ThCl₂·2LiCl·2DME

empirical formula	C ₂₈ H ₅₀ Cl ₄ Li ₂ O ₄ SiTh·0.5(C ₄ H ₁₀ O) ₂
fw	911.55
temperature	200(2) K
wavelength	0.71073 Å
cryst syst, space group	monoclinic, <i>P</i> 2 ₁ / <i>n</i>
	<i>a</i> = 17.8040(10) Å, α = 90°
	<i>b</i> = 20.0580(10) Å, β = 90.610(10)°
	<i>c</i> = 21.9350(10) Å, γ = 90°
unit cell dimens	
volume	7832.8(17) Å ³
<i>Z</i> , calcd density	8, 1.546 Mg/m ³
abs coeff	4.143 mm ⁻¹
<i>F</i> (000)	3624
cryst size	0.15 × 0.22 × 0.31 mm
θ range for data collection	1.78 to 26.73°
limiting indices	0 ≤ <i>h</i> ≤ 22, 0 ≤ <i>k</i> ≤ 25, –27 ≤ <i>l</i> ≤ 27
no. of reflns collected/ unique	16 590/16 590 [<i>R</i> (int) = 0.0000]
completeness to highest θ	99.8%
refinement method	full-matrix least-squares on <i>F</i> ²
no. of data/restraints/ params	16590/0/448
goodness-of-fit on <i>F</i> ²	1.020
final <i>R</i> indices [<i>I</i> > 2σ(<i>I</i>)]	<i>R</i> 1 = 0.0563, w <i>R</i> 2 = 0.1309
<i>R</i> indices (all data)	<i>R</i> 1 = 0.0972, w <i>R</i> 2 = 0.1510
largest diff peak and hole	31.172 and –1.578 e Å ⁻³

flask. The Schlenk was heated in a thermostatic oil bath at 80 °C for 21 days, yielding 98% conversion of the 1-octene into products. When no other changes were observed in the ¹H NMR, the reaction was stopped and all the volatiles were transferred into a new Schlenk flask. The products were identified by comparing their retention times in a GC chromatograph to commercially available octenes (*E*-2-octene, *E*-3-octene, and *E*-4-octene). Other products were obtained as described in the literature.⁹ The product percentage ratio was determined from the relative peak areas in GC and normalized, yielding in their order of appearance 1-octene (2.0%), *E*-4-octene (3.8%), *E*-3-octene (39.4%), *E*-2-octene (13.0%), and *Z*-2-octene (41.8%).

(9) Isomerization Reaction of *E*-2-Octene. As described above, the same reaction was carried out with *E*-2-octene for the same amount of time, yielding 17.8% conversion. The product ratio among the products was found to be *E*-3-octene (11.2%), *E*-2-octene (82.2%), and *Z*-2-octene (6.6%).

X-ray Crystallographic Measurements. A single dark crystalline prism immersed in Parathone-N oil was quickly fished with a capillary tube and mounted on a Kappa CCD diffractometer under a cold stream of nitrogen at 200 K. Data collection was performed using monochromatized Mo Kα radiation using omega scans and phi scans to cover the Ewald sphere.¹⁰ Accurate cell parameters were obtained with 57 516 reflections.¹¹ The structure was solved by SHELXS97 direct methods¹² and refined by the SHELXL97 program package.¹³ The Th, Si, and Cl atoms of the complex molecule were refined anisotropically, but the Li, C, and O atoms only isotropically. No hydrogens were included in the refinement because of their rather low contribution. Software used for molecular graphics: ORTEP, TEXRAY Structure Analysis package.¹⁴ Cell parameters and refinement data are presented in Table 1.

(9) (a) Averbuj, C.; Eisen, M. S. *J. Am. Chem. Soc.* **1999**, *121*, 8755. (b) Volkis, V.; Shmulinson, M.; Averbuj, C.; Lisovskii, A.; Edelmann, F. T.; Eisen, M. S. *Organometallics* **1998**, *17*, 3155.

(10) Nonius, Kappa CCD Server Software; Nonius BV: Delft, The Netherlands, 1997.

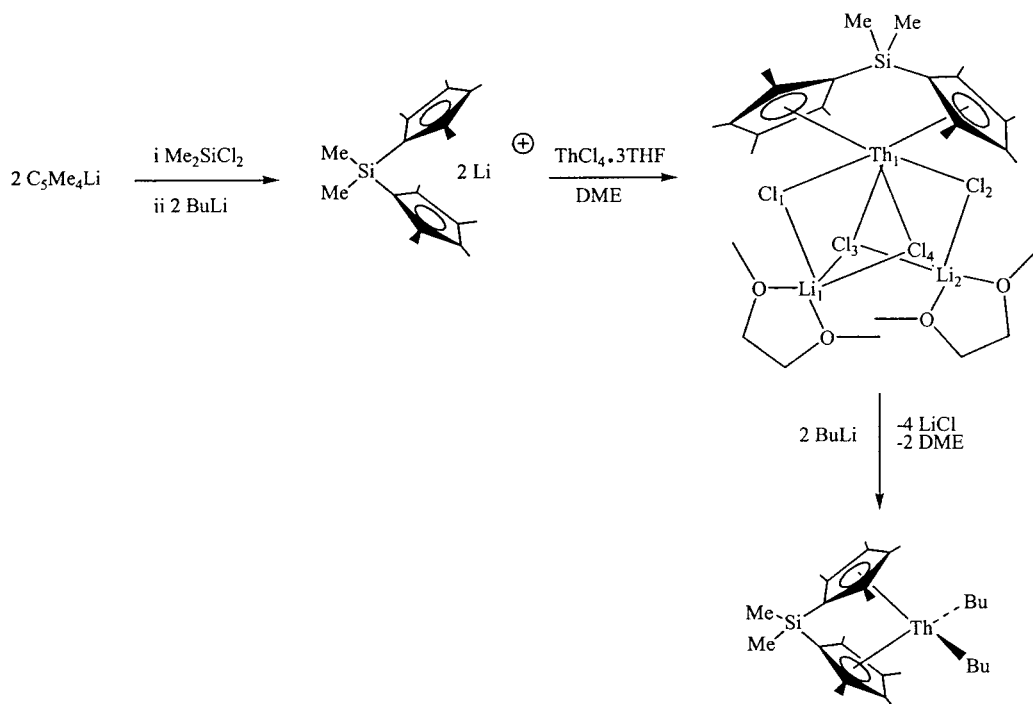
(11) Otwinowski, Z.; Minor, W. *Methods Enzymol.* **1997**, *276*, 307.

(12) Sheldrick, G. M. *Acta Crystallogr.* **1990**, *A46*, 467.

(13) Sheldrick, G. M. *SHELXL97*, Program for the Refinement of Crystal Structures; University of Göttingen, Germany, 1997.

(14) ORTEP, TEXRAY Structure Analysis Package; Molecular Structure Corporation, 3200 Research Forest Dr., The Woodlands, TX, 1999.

Scheme 1. Pathway Followed for the Synthesis of the Coordinative Unsaturated Complex $\text{Me}_2\text{SiCp}''_2\text{Th}^n\text{Bu}_2$



Results

The goal of this investigation was to examine the scope, chemoselectivity, regioselectivity, ancillary ligand sensitivity, kinetics, and thermodynamic studies for a number of processes catalyzed by organothorium complexes. The research focused on a comparison between two different ligations: the normal C_5Me_5 (Cp^*) and the *ansa*-type bridge ligation $\text{Me}_2\text{SiCp}''_2$ ($\text{Cp}'' = \text{C}_5\text{Me}_4$) for the oligomerization of terminal alkynes and the hydrosilylation of alkynes and alkenes with PhSiH_3 . This study represents an extension of the unique reactivities of organoactinide complexes with terminal alkynes with or without the presence of primary silanes. In addition, we present a complementary comparison for the organoactinides in the novel hydrosilylation of alkenes. The three catalytic processes here reported, for the coordinative unsaturated bridged complex, are interrelated due to a unique kinetic behavior—an inverse kinetic order—in the olefin, (or alkyne) stimulating a full study for each reaction and presenting them together to contribute to a broad understanding of this organoactinide chemistry. In the following presentation of the results we focus on the reaction scope, alkyne or alkene substituent, ligand effect, kinetics, and the rate law expressions. In addition we report on the solid-state characterization of the starting organothorium complex, the bridged $\text{Me}_2\text{SiCp}''_2\text{ThCl}_2$, an intermediate to the synthesis of the precatalysts $\text{Me}_2\text{SiCp}''_2\text{Th}^n\text{Bu}_2$,¹⁵ allowing a structural comparison with $\text{Cp}^*_2\text{ThCl}_2$ ¹⁶ and $\text{Cp}^*_2\text{ThMe}_2$. Furthermore, we present D_2O quenching experiments between an organoactinide and an olefin, allowing the indirect formulation of a π -alkene–Th–

alkyl complex, a key intermediate in the hydrosilylation of alkenes. We start the results with the reaction scope for the bridged-organactinide-catalyzed chemo- and regioselective dimerization of alkynes, followed by the reactivity in the selective hydrosilylation of terminal alkynes and alkenes with phenylsilane. In the latter alkene process the studies with the organoactinide $\text{Cp}^*_2\text{ThMe}_2$ are also presented.

Synthesis of $\text{Me}_2\text{SiCp}''_2\text{ThCl}_2$ and $\text{Me}_2\text{SiCp}''_2\text{Th}^n\text{Bu}_2$. The complete syntheses of the complexes $\text{Me}_2\text{SiCp}''_2\text{ThCl}_2$ and $\text{Me}_2\text{SiCp}''_2\text{Th}^n\text{Bu}_2$ have been performed similarly to those reported in the literature (Scheme 1).^{3c,17} The complex $\text{Me}_2\text{SiCp}''_2\text{ThCl}_2$ was isolated in 82% yield, and the reducing steric bulk of the chelating ligand results in the isolation of the lithium chloride adducts, as observed for analogous uranium complex although with different adducted solvent.¹⁷ The single-crystal X-ray diffraction (Figure 3, Tables 1 and 2) reveals a typical bent metallocene complex. The ring–centroid–Th–centroid angle (113.3°) is significantly smaller than that observed in unhindered bis(pentamethylcyclopentadienyl) thorium complexes (130 – 138°),^{16,18} is also slightly smaller than the angle determined for the bridged thorium dialkyl complex $[\text{Me}_2\text{SiCp}''_2\text{Th}(\text{CH}_2\text{Si}(\text{CH}_3)_3)_2]$ (118.4°),^{3c} and is comparable to the analogous uranium complex $[\text{Me}_2\text{SiCp}''_2\text{U}(\mu\text{-Cl})\{\text{Li}(\text{TMEDA})\}_2]$.¹⁷ The thorium–carbon (carbon = Cp'' ring carbons) bond lengths are not equidistant, having a shorter distance between the metal and the first carbon adjacent to the silicon bridge. This spreading of M–C bond distances has been reported for other metallocene complexes and is assumed to be a result of the strain generated by the Me_2Si bridge.¹⁹ Interestingly, two of

(15) The preparation of $\text{Me}_2\text{SiCp}''_2\text{Th}^n\text{Bu}_2$ and $\text{Me}_2\text{SiCp}''_2\text{ThCl}_2$ has been reported, but the crystal structure of the latter has not been reported yet.^{3c}

(16) Spirlet, M. R.; Rebizant, J.; Apostolidis, C.; Kanellakopulos, B. *Acta Crystallogr.* **1992**, *C48*, 2135.

(17) For similar organouranium complexes, see: Schnabel, R. C.; Scott, B. L.; Smith, W. H.; Burns, C. J. *J. Organomet. Chem.* **1999**, *591*, 14.

(18) Bruno, J. W.; Smith, G. M.; Marks, T. J. *J. Am. Chem. Soc.* **1986**, *108*, 40.

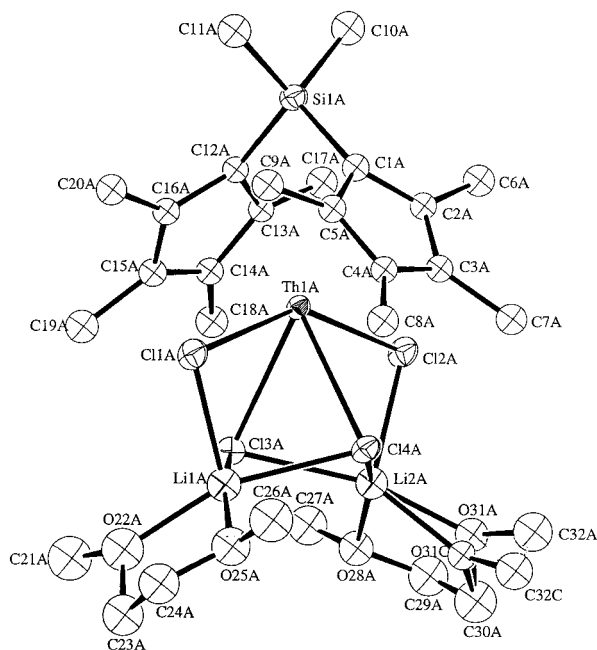


Figure 3. Perspective ORTEP drawing of the non-hydrogen atoms in complex $\text{Me}_2\text{SiCp}^*_2\text{ThCl}_2 \cdot 2\text{LiCl} \cdot 2\text{DME}$. All atoms are represented by thermal ellipsoids drawn to encompass 50% of the electron density, showing ellipsoids at 50% probability.

Table 2. Bond Lengths (Å) and Angles (deg) for Complex $\text{Me}_2\text{SiCp}^*_2\text{ThCl}_2 \cdot 2\text{LiCl} \cdot 2\text{DME}$

Th(1A)–Cl(1A)	2.770(2)
Th(1A)–Cl(2A)	2.761(2)
Th(1A)–Cl(3A)	2.950(2)
Th(1A)–Cl(4A)	2.918(2)
Th(1A)–C(1A)	2.792(9)
Th(1A)–C(2A)	2.834(9)
Th(1A)–C(3A)	2.882(9)
Th(1A)–C(4A)	2.892(9)
Th(1A)–C(5A)	2.815(9)
Th(1A)–C(12A)	2.780(8)
Th(1A)–C(13A)	2.805(8)
Th(1A)–C(14A)	2.900(9)
Th(1A)–C(15A)	2.922(9)
Th(1A)–C(16A)	2.848(9)
Cl(1A)–Li(1A)	2.404(19)
Cl(3A)–Li(1A)	2.46(2)
Cl(4A)–Li(1A)	2.526(19)
Cl(2A)–Li(2A)	2.396(18)
Cl(3A)–Li(2A)	2.504(18)
Cl(4A)–Li(2A)	2.509(18)
Cl(2A)–Th(1A)–Cl(1A)	146.66(7)
Cl(1A)–Th(1A)–Cl(3A)	76.17(7)
Cl(2A)–Th(1A)–Cl(3A)	76.07(7)
Cl(3A)–Th(1A)–Cl(4A)	65.94(7)
Cl(2A)–Th(1A)–Cl(4A)	76.12(7)
Cl(1A)–Th(1A)–Cl(4A)	75.93(7)
Li(1A)–Cl(1A)–Th(1A)	86.5(5)
Li(2A)–Cl(2A)–Th(1A)	87.0(4)
Li(1A)–Cl(3A)–Li(2A)	95.1(6)
Li(1A)–Cl(3A)–Th(1A)	81.6(4)
Li(2A)–Cl(3A)–Th(1A)	81.1(4)
Li(2A)–Cl(4A)–Li(1A)	93.5(6)
Li(2A)–Cl(4A)–Th(1A)	81.6(4)
Li(1A)–Cl(4A)–Th(1A)	81.2(4)

the thorium–chloride bonds are shorter than the other two. $\text{Th}(1)\text{–Cl}(1) = 2.770(2)$ Å, $\text{Th}(1)\text{–Cl}(2) = 2.661(2)$ Å, $\text{Th}(1)\text{–Cl}(3) = 2.950(2)$ Å, and $\text{Th}(1)\text{–Cl}(4) = 2.918(2)$

(19) Bajgur, C. S.; Tikkanen, W. R.; Petersen, J. L. *Inorg. Chem.* **1985**, *24*, 2539.

Å. The longer Th–Cl distances are those corresponding to the chlorine atoms disposed in the 3-fold bridging positions and coordinated to both lithium atoms. Each of other two chlorine atoms is coordinated only to one lithium atom. All the Th–Cl distances are longer than those observed for terminal Th–Cl distances ($\text{Th}\text{–Cl} = 2.601$ Å for $\text{Cp}^*_2\text{ThCl}_2$ or 2.65 for $\text{Cp}^*_2\text{Th}(\text{Cl})\text{Me}$),²⁰ but similar to the analogous uranium complex.¹⁷ The Li–Cl bond lengths and Li–O bond lengths are similar to those found in other organometallic complexes.²¹

Scope of $\text{Me}_2\text{SiCp}^*_2\text{Th}^n\text{Bu}_2$ -Catalyzed Dimerization of Terminal Alkynes. The bridged organoactinide complex $\text{Me}_2\text{SiCp}^*_2\text{Th}^n\text{Bu}_2$ is a precatalyst for the chemo- and regioselective dimerization of terminal alkynes. The reaction of $\text{Me}_2\text{SiCp}^*_2\text{Th}^n\text{Bu}_2$ with a large excess of a terminal alkyne (benzene, alkyne/catalyst ratio up to 2000:1), at room temperature, results in the regioselective formation of the head-to-tail geminal dimer (Table 3). By performing the reaction at a higher temperature (78 °C), the geminal dimer was produced rapidly, although for some specific alkynes ($^i\text{PrC}\equiv\text{CH}$ and $^n\text{BuC}\equiv\text{CH}$) minor amounts of the specific head-to-tail-to-tail trimer (up to 5%) were also observed (eq 5). The catalytic reaction proceeds, in most cases, until completion at the corresponding temperatures, which were followed by either GC or GC/MS and ^1H NMR spectroscopy. For the low-boiling alkyne ($\text{MeC}\equiv\text{CH}$, $^i\text{PrC}\equiv\text{CH}$), a heavy glass high-pressure J-Young Schlenk flask was used. All the products were characterized by ^1H NMR, ^{13}C NMR, and 2D-NMR spectroscopy, GC/MS, high-resolution mass spectroscopy, and microanalysis or by comparison to literature $^1\text{H}/^{13}\text{C}$ NMR spectral data and data from authentic samples prepared according to literature procedures. Isolation protocols for the products involved high-vacuum transfer of the products and volatiles with the subsequent elimination of the solvent and final distillation of the products or purification by silica gel column chromatography.

The dimerization results presented in Table 3 show that the higher the temperature, the faster the dimerization is obtained. Although no large difference is observed among similar alkyne substituents, the dimerization reaction of either $^i\text{PrC}\equiv\text{CH}$ or $^n\text{BuC}\equiv\text{CH}$ with $\text{Me}_2\text{SiCp}^*_2\text{Th}^n\text{Bu}_2$ is by far much faster and selective than the dimerization with $\text{Cp}^*_2\text{ThMe}_2$ (compare entries 4 and 5 or 8 and 9 in Table 3). The most striking result regarding the dimerization/oligomerization of terminal alkynes was found for $(\text{TMS})\text{C}\equiv\text{CH}$ ($\text{TMS} = \text{Me}_3\text{Si}$). When performing the dimerization at room or high temperature, no catalytic reaction was observed by using the bridged complex (butane is evolved), in contrast to the results obtained in the reaction of $(\text{TMS})\text{C}\equiv\text{CH}$ with $\text{Cp}^*_2\text{ThMe}_2$, in which the geminal dimer (10%) and the head-to-tail-to-head trimer (90%) are obtained with high regioselectivity.²² Interestingly, the chemical and thermal stability of the organoactinide compound was studied by performing the dimerization

(20) Straub, T.; Haskel, A.; Neyroud, T. G.; Kapon, M.; Botoshansky, M.; Eisen, M. S. Submitted for publication.

(21) (a) Dashti-Mommertz, A.; Neumuller, B. *Z. Anorg. Allg. Chem.* **1999**, *625*, 954. (b) Qian, C.; Nie, W.; Sun, J. *J. Chem. Soc., Dalton Trans.* **1999**, 3283. (c) Pauls, J.; Neumuller, B. *Z. Anorg. Allg. Chem.* **2000**, *626*, 270. (d) Heine, A.; Stalke, D. *Angew. Chem., Int. Ed. Engl.* **1993**, *32*, 121.

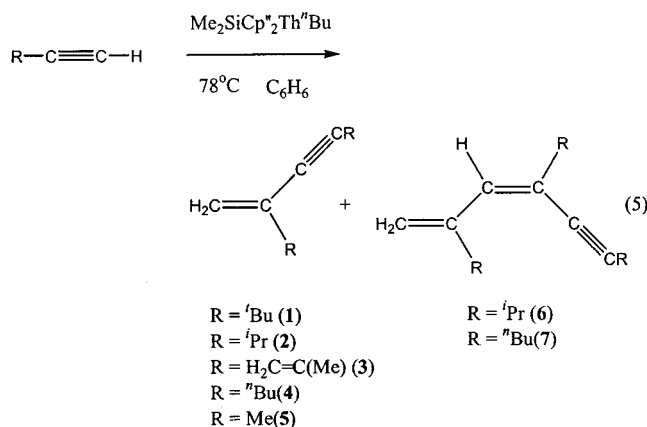
(22) Straub, T.; Haskel, A.; Eisen, M. S. *J. Am. Chem. Soc.* **1995**, *117*, 6364.

Table 3. Activity Data for the Dimerization of Terminal Alkynes Promoted by $\text{Me}_2\text{SiCp}^*_2\text{Th}^n\text{Bu}_2$ ^a

entry	cat. ^b	R in $\text{RC}\equiv\text{CH}$	temp [°C]	time [h]	yield of <i>gem</i> -dimer [%]	N_t [h^{-1}]	ref
1	B	^t Bu	20	36	18	4.1	this work
2	B	^t Bu	78	2	42	175	this work
3	B	ⁱ Pr	20	120	85	7.1	this work
4	B	ⁱ Pr	78	2	93(5) ^c	426	this work
5	NB	ⁱ Pr	78	22	1	0.04	5
6	B	$\text{H}_2\text{C}=\text{C}(\text{Me})$	20	45	78	37	this work
7	B	$\text{H}_2\text{C}=\text{C}(\text{Me})$	78	2	33(34) ^d	760	this work
8	B	ⁿ Bu	78	2	92(4) ^c	420	this work
9	NB	ⁿ Bu	78	16	39	2.0	5
10	B	Me	78	48	64	1.5	this work

^a Solvent = benzene. ^b B = $\text{Me}_2\text{SiCp}^*_2\text{Th}^n\text{Bu}_2$, NB = $\text{Cp}^*_2\text{ThMe}_2$. ^c The numbers in parentheses correspond to the head-to-tail-to-head trimer. ^d The numbers in parentheses correspond to the [4+2] intermolecular Diels–Alder adduct.

of **2** in 10 consecutive runs. The reactions were performed by adding always the same amount of $\text{}^i\text{PrC}\equiv\text{CH}$ to the reaction mixture, allowing the production of the dimer without losing the catalyst activity. This result indicates that in the absence of moisture or oxygen this complex is fairly stable.



The dimerization of the alkene-functionalized alkyne produces dimer **3**, which undergoes an intermolecular Diels–Alder cyclization at room temperature, in moderate yields, or cyclizes quantitatively either by refluxing a benzene solution containing the purified compound **3** or by heating compound **3** in the reaction mixture without any prepurification (eq 6).

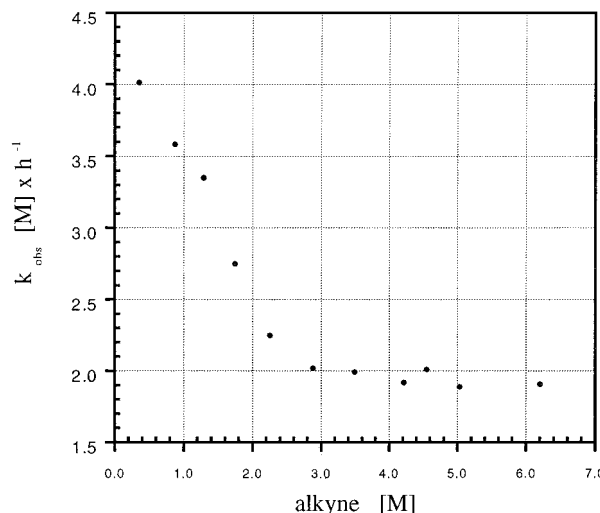
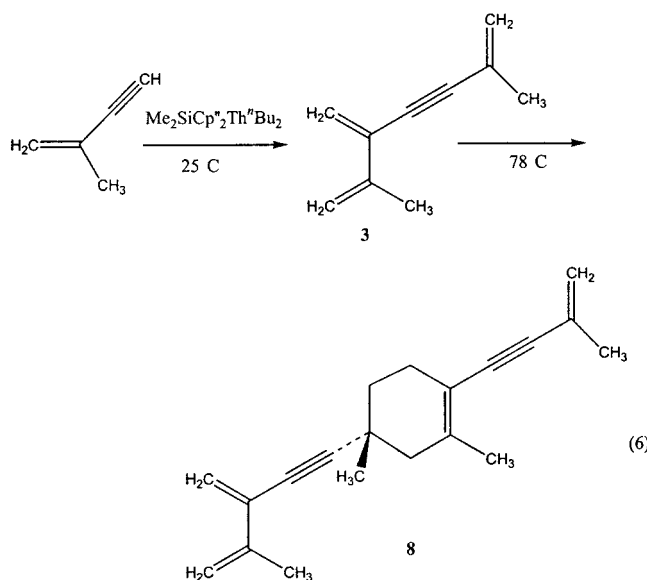


Figure 4. Determination of the reaction order in alkyne concentration for the dimerization of $\text{}^i\text{PrC}\equiv\text{CH}$ mediated by $\text{Me}_2\text{SiCp}^*_2\text{Th}^n\text{Bu}_2$ as the pre-catalyst in benzene- d_6 at 25 °C exhibiting two domain regions.

Kinetic Studies of the Dimerization of Terminal Alkynes. Kinetically, the catalytic reaction of $2 \text{}^i\text{PrC}\equiv\text{CH} \rightarrow \mathbf{2}$ promoted by $\text{Me}_2\text{SiCp}^*_2\text{Th}^n\text{Bu}_2$ was undertaken by in-situ ^1H NMR spectroscopy. The reaction of a ~ 100 -fold excess of alkyne was monitored with constant substrate concentrations until complete substrate consumption. The disappearance of the terminal alkynes' hydrogen $\text{C}\equiv\text{CH}$ ($\delta = 2.28$ ppm) and the appearance of the vinylic $\text{CH}_2=\text{CR}$ ($\delta = 5.35$ ppm) ^1H resonances were normalized. The turnover frequency of the reaction was calculated from the slope of the kinetic plots of substrate-to-catalyst ratio vs time. When the initial concentration of the terminal alkyne is held constant and the concentration of the catalytic precursor is varied over a ~ 25 -fold concentration range, a plot of reaction rate vs pre-catalyst concentration indicates that the reaction is first-order dependent in pre-catalyst in analogy to the oligomerization of terminal alkynes promoted by $\text{Cp}^*_2\text{-AnMe}_2$.^{5a} This result indicates that the best formulation of the active species in solution should be monomeric. When the concentration of the catalyst is maintained constant, and the concentration of the alkyne is varied over a ~ 15 -fold concentration range, a plot of the reaction rate vs alkyne concentration exhibits two domains of behavior (Figure 4). At low concentrations, an inverse proportionality is observed indicating that the reaction is in an inverse first order, and at higher

Table 4. Activity Data for the Hydrosilylation of Terminal Alkynes with PhSiH₃ Promoted by Me₂SiCp''₂ThⁿBu₂^a

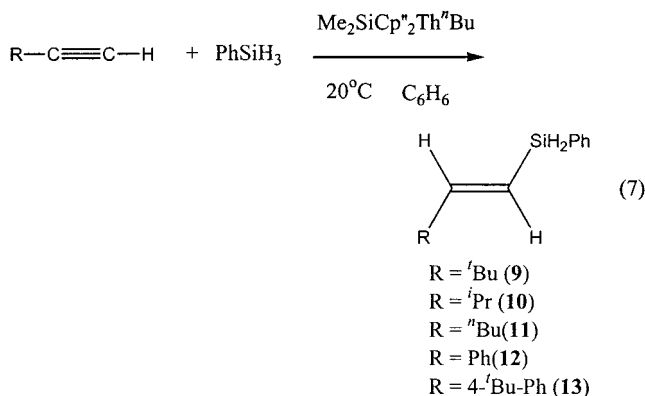
entry	cat. ^b	R in RC=CH	temp [°C]	time [h]	yield of		ref
					<i>trans</i> -RCH=CHSiH ₂ Ph	N _t [h ⁻¹]	
1	B	^t Bu	20	0.25	90	677	this work
2	B	^t Bu	20	0.5	98		this work
3	NB	^t Bu	20	24	48	0.7	6
4	B	ⁱ Pr	20	0.3	92	504	this work
5	NB	ⁱ Pr	20	24	42	0.6	6
6	B	ⁿ Bu	20	0.25	96	475	this work
7	B	Ph	20	1	89	1089	this work
8	B	4- ^t BuPh	20	2.5	93	270	this work
9	B	H ₂ C=C(Me)	20	1	95	65	this work

^a Solvent = benzene. ^b B = Me₂SiCp''₂ThⁿBu₂, NB = Cp''₂ThMe₂.

concentrations, the reaction exhibits a zero order in alkyne. An inverse proportionality in catalytic systems is well known and consistent with an equilibrium before the rate-limiting step.^{23a,b} The change from an inverse rate to a zero rate is consistent with two equilibrium processes. One of these equilibrium processes is routing the complex *out of the catalytic cycle* (inverse order), whereas the second equilibrium is the rate-determining step toward the dimer formation palpable only at higher alkyne concentrations. A similar alkyne behavior has been already observed in the oligomerization of terminal alkynes with the highly reactive unsaturated uranium cationic complex [(Et₂N)₃U][BPh₄].²⁴ For Me₂SiCp''₂ThⁿBu₂, a similar kinetic dependence is observed on alkyne and catalysts over a 40–80 °C temperature range. The derived activation parameters *E*_a, Δ*H*[‡], and Δ*S*[‡] from an Eyring analysis are 11.7(3) kcal mol⁻¹, 11.0(3) kcal mol⁻¹, and –22.6(5) eu, respectively.^{23a} The negative Δ*S*[‡] value indicates a highly ordered four-centered transition state for the insertion of the alkyne into the metal–carbonyl bond.

Catalytic Hydrosilylation of Terminal Alkynes.

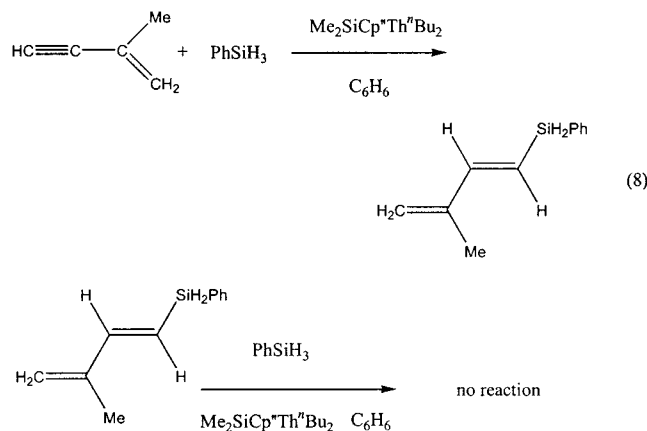
The reaction of Me₂SiCp''₂ThⁿBu₂ with an excess of a terminal alkyne and PhSiH₃ (benzene, PhSiH₃/alkyne/catalyst ratio 150:150:1), at room temperature, results in the extremely rapid and regioselective formation of the hydrosilylation *trans*-vinylsilane as the unique product regardless of the alkyne substituent (eq 7) (Table 4).



(23) (a) See: Supporting Information for the respective kinetic plots. (b) Straub, T. R., G.; Frank, W.; Eisen, M. S. *J. Chem. Soc., Dalton Trans.* **1996**, 2541. (c) Eisen, M. S.; Straub, T.; Haskel, A. *J. Alloys Compd.* **1998**, 271, 116.

(24) (a) Wang, J. Q.; Dash, A.; Berthet, J. C.; Ephritikhine, M.; Eisen, M. S. *Organometallics* **1999**, 18, 2407. (b) Dash, A. K.; Wang, J. X.; Berthet, J. C.; Ephritikhine, M.; Eisen, M. S. *J. Organomet. Chem.* **2000**, 604, 83.

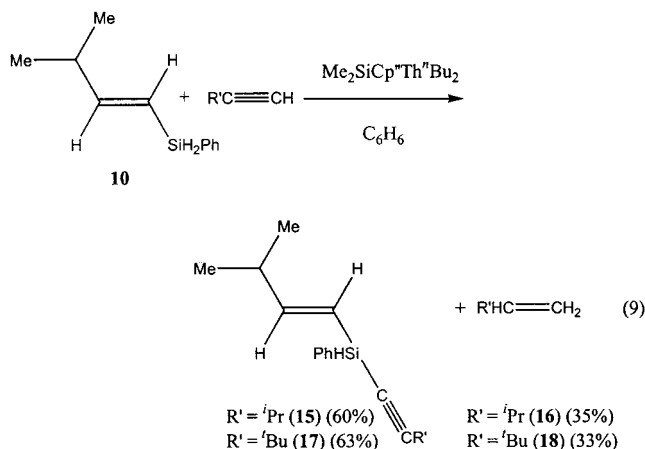
When the olefin-functionalized alkyne was used for the reaction with PhSiH₃, the alkyne moiety was regioselectively hydrosilylated toward the corresponding *trans*-diene **14** (no *cis*-isomer was observed), corroborating that the metathesis reaction with an organo-f-complex (An-R) ensues via a concerted four-centered transition state disposing the An–R moieties at the product in a *syn*-stereochemistry. After the quantitative formation of the *trans*-vinylsilane, addition of an excess of PhSiH₃ to the reaction mixture did not induce subsequent hydrosilylation on any of the two olefinic moieties in **14** neither at low nor at high temperatures (eq 8), indicating the large difference in reactivities between the triple bond and the double bond toward the *ansa*-organoactinide.



It is noteworthy that by adding an excess of PhSiH₃ to any of the vinylsilane products (**9**–**13**) the formation of new compounds was not observed. However, addition of a second equivalent of an alkyne to a hydrosilylation product allows the formation of the corresponding alkene and the dehydrogenative coupling of the alkyne with the *trans*-vinylsilane (eq 9).²⁵ The addition of the second alkyne to the hydrosilylated product can be equal to or different from the starting alkyne used for the

(25) For dehydrogenative coupling of silane references, see: (a) Forsyth, C. M.; Nolan, S. P.; Marks, T. J. *Organometallics* **1991**, 10, 2543. (b) Watson, P. L.; Tebbe, F. N. U.S. Patent 4,965,386, 1990. (c) Tilley, T. D. *Acc. Chem. Res.* **1993**, 26, 22, and references therein. (d) Corey, J. Y.; Huhmann, J. L.; Zhu, X.-H. *Organometallics* **1993**, 12, 1121, and references therein. (e) Woo, H.-G.; Walzer, J. F.; Tilley, T. D. *J. Am. Chem. Soc.* **1992**, 114, 7047. (f) Harrod, J. F. In *Inorganic and Organometallic Polymers with Special Properties*; Lain, R. M., Ed.; Kluwer Academic Publishers: Amsterdam, 1991; Chapter 14, and references therein. (g) Kobayashi, T.; Sakakura, T.; Hayashi, T.; Yumura, M.; Tabaka, M. *Chem. Lett.* **1992**, 1157. (h) Aitken, C.; Barry, J. P.; Gauvin, F. G.; Harod, J. F.; Malek, A.; Rousseau, D. *Organometallics* **1989**, 8, 1732.

production of the vinylsilane. This result indicates that the vinylsilane products are not in equilibrium with the starting materials. In addition, secondary silanes are unable to undergo a metal-catalyzed second hydrosilylation reaction forming a Si–C(sp²) bond but have a preference to undergo a dehydrogenative coupling with a terminal alkyne producing a Si–C(sp) bond.



Kinetic Studies of the Hydrosilylation of Terminal Alkynes with Primary Silanes. Kinetic measurements on the hydrosilylation of a ~150-fold excess of ⁱPrC≡CH with PhSiH₃ catalyzed by Me₂SiCp''₂ThⁿBu₂ were also undertaken by in-situ ¹H NMR spectroscopy. The reaction was monitored with constant substrate concentrations until complete substrate consumption. The disappearance of the terminal alkynes' hydrogen C≡CH (δ = 2.28 ppm) and the appearance of the vinylic CH=CHSi (δ = 6.31 and 5.62 ppm) ¹H resonances were normalized. The turnover frequency of the reaction was calculated from the slope of the kinetic plots of substrate-to-catalyst ratio vs time. Considering the rapidity of the actinide–alkane protonolysis by primary silanes,²⁴ it seems unreasonable that the formation of a thorium–hydride could be a turnover-limiting step under most catalytic conditions. We have found that, under the reaction conditions, for both complexes Me₂SiCp''₂ThⁿBu₂ and Cp*₂ThMe₂, stoichiometric amounts of PhSiH₂Bu and PhSiH₂Me are rapidly obtained, respectively. This result corroborates that a rapid metathesis between the precatalysts and the silane is operative, forming the corresponding hydride complexes. When the initial concentration of the alkyne and the silane are maintained constant and the concentration of the catalytic precursor is varied over a ~13-fold concentration range, a plot of the reaction rate vs precatalyst concentration indicates that the reaction is first-order dependent on precatalyst.^{23a} When the concentration of the alkyne and the catalyst are held constant and the concentration of the silane is changed over a ~10-fold concentration range, a plot of the reaction rate vs precatalyst concentration indicates that the reaction is first-order dependent on silane.^{23a} When the concentration of the silane and catalyst are maintained constant and the alkyne concentration is changed over a ~42-fold concentration range (Figure 5) a plot of the reaction rate vs alkyne concentration exhibits an inverse proportionality, indicating that the reaction is inverse first order dependent on alkyne. The inverse proportionality is consistent with a rapid equilibrium

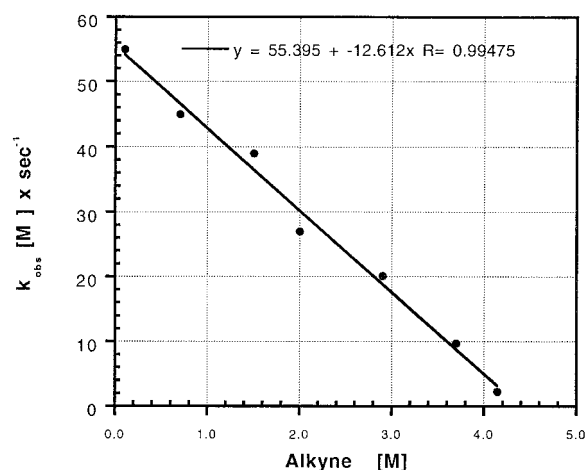


Figure 5. Determination of the reaction order in alkyne concentration for the hydrosilylation of ⁱPrC≡CH with PhSiH₃ mediated by Me₂SiCp''₂ThⁿBu₂ as the precatalyst in benzene-*d*₆ at 20 °C. The line represents the least-squares fit to the data points.

before the turnover-limiting step, routing one of the key organoactinide intermediates out of the catalytic cycle. Thus, the rate law for the hydrosilylation of terminal alkynes with PhSiH₃ promoted by Me₂SiCp''₂ThⁿBu₂ can be formulated as presented in eq 10.

$$v = k[\text{Me}_2\text{SiCp}''_2\text{Th}^n\text{Bu}_2][\text{silane}]^1[\text{alkyne}]^{-1} \quad (10)$$

The derived ΔH^\ddagger and ΔS^\ddagger parameter values (error values are in parentheses) from a thermal Eyring analysis are 10.07(5) kcal mol⁻¹ and -22.06(5) eu, respectively.^{23a}

It is worth mentioning at this stage the difference in the kinetic behavior of the alkyne substrate in the hydrosilylation reaction as compared to the dimerization process. In the latter process, the alkyne is plausibly operative in two parallel routes, both sensitive to the alkyne concentration. In one reaction pathway the alkyne exhibits an inverse kinetic order (routing out one of the active compounds from the catalytic cycle), whereas in the second pathway the alkyne is reacting in the rate-determining step. Thus, the effect only at high alkyne concentrations nulls the overall alkyne effect. In the earlier hydrosilylation process, the alkyne is only routing an active compound out of the catalytic cycle and the silane is reacting in the rate-limiting step. Thus no annulment of the alkyne effect is observed.

Mechanistically, in the hydrosilylation reactions of organo-f-element complexes two Chalk–Harrod mechanisms have been proposed as plausible routes, except for the inclusion of a σ -bond metathesis instead of the classical oxidative addition–reductive elimination processes. The two mechanisms differ in the reactive intermediates; the hydride (M–H) route and the silane (M–SiR₃) route.^{7a,26,27} The use of terminal alkynes, for bridged organoactinides, is an excellent probe to investigate which of the two routes is the major followed pathway. Thus, taking into account that the alkyne will insert with the substituent group pointing away from the metal center (as observed in the dimerization), if the hydrosilylation reaction goes through an M–SiR₃ intermediate, the *gem*-hydrosilylated vinyl isomer will

Table 5. Activity Data for the Hydrosilylation of Alkenes Promoted by Cp*₂ThMe₂ and Me₂SiCp''₂ThⁿBu₂^a

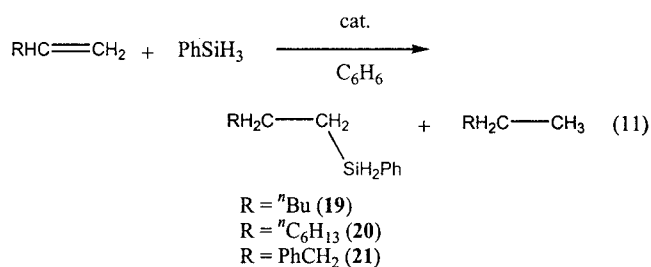
entry	cat. ^b	R in RHC=CH	temp [°C]	time [h]	yield of		N _t ^c [h ⁻¹]
					1-silylalkane [%]	yield of alkane [%]	
1	NB	ⁿ Bu	20	12	54	44	1.5
2	B	ⁿ Bu	20	12	63	35	5.5
3	NB	ⁿ Bu	78	6	57	41	3.2
4	B	ⁿ Bu	78	1	62	36	64.5
5	NB	ⁿ C ₆ H ₁₃	20	12	68	30	1.9
6	B	ⁿ C ₆ H ₁₃	20	12	65	33	4.6
7	NB	PhCH ₂	78	6	61	38	4.8
8	B	PhCH ₂	78	1	71	29	83.1
9	NB	Ph	78	36	65(6) ^d	28	0.9
10	B	Ph	78	36	31(30) ^d	37	1.9

^a Solvent = benzene. ^b B = Me₂SiCp''₂ThⁿBu₂, NB = Cp*₂ThMe₂. ^c Turnover frequency for the hydrosilylation process. ^d The numbers in parentheses correspond to the 2,1-addition hydrosilylation product, 2-(phenylsilyl)ethylbenzene.

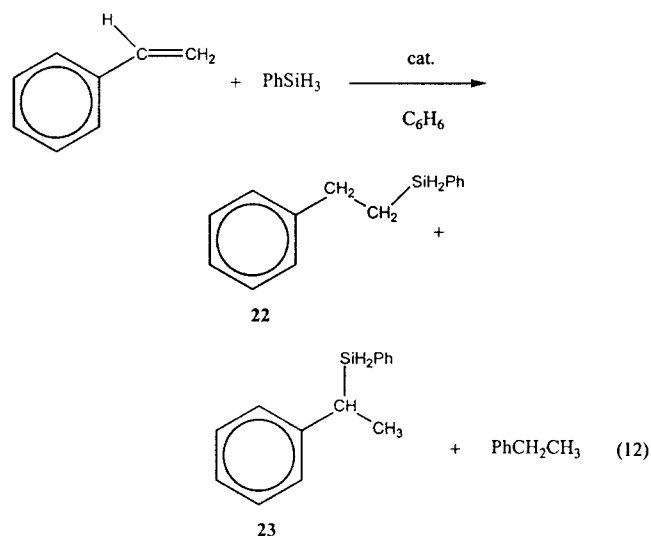
be formed, whereas through the M–H route only the *trans*-isomer will be obtained (if the insertion stereochemistry is not maintained, the *cis* product will be also observed). The exclusive selectivity obtained for Me₂-SiCp''₂ThⁿBu₂ toward the *trans*-hydrosilylated isomer argues that the hydride route is acting as the major mechanistic pathway. Although no organometallic complexes containing a Th–Si have been characterized presumably due to its low bond energy,²⁸ we cannot rule out this pathway due to the dehydrogenative coupling of the vinylsilane and the terminal alkyne, although if operative, this is not the major pathway in the hydrosilylation reaction but may be partially operative in the dehydrogenative coupling.

Scope on the Catalytic Hydrosilylation of Alkenes Promoted by the Organoactinide Complexes Cp*₂ThMe₂ and Me₂SiCp''₂ThⁿBu₂. The organoactinide complexes Cp*₂ThMe₂ and Me₂SiCp''₂ThⁿBu₂ were found to be good precatalysts for the highly regioselective hydrosilylation of alkenes. The chemoselectivity of the reactions was moderate since the hydrogenated alkane was always encountered as a concomitant product, although is extremely simple to purify the reaction mixture by separating an alkane (Table 5). Hence, the reactions of Cp*₂ThMe₂ and Me₂SiCp''₂

ThⁿBu₂ with an excess of an alkene and PhSiH₃, at room temperature, results in the formation of the regioselective 1,2-addition hydrosilylated alkene and an alkane with no major differences between the two organoactinides (eq 11).



Since for the substrate allyl benzene, compound **21** was the only hydrosilylated product, it was important to compare the effect of distance between the aromatic ring and the metal center. It seems to us rather plausible to expect a fine-tuning of the product toward the 2,1-addition hydrosilylation product by the possible aromatic ring interaction with the electropositive metal center. Thus, in the hydrosilylation of styrene with each of the organoactinides (eq 12) both 1,2- and 2,1-addition hydrosilylation products are obtained, as expected, in addition to ethylbenzene. For Cp*₂ThMe₂ a small amount of compound **23** (6%) was obtained, whereas for the coordinative unsaturated complex Me₂SiCp''₂ThⁿBu₂ equal amounts of both isomers **22** and **23** were yielded (entries 9, 10 in Table 5).

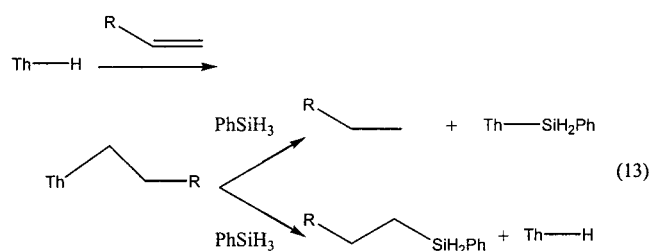


(26) (a) Ojima, I.; Li, Z.; Zhu, J. In *The Chemistry of Organic Silicon Compounds*; Rappoport, S., Apeloig, Y., Eds.; Wiley: New York, 1998; Chapter 29, and references therein. (b) Reichl, J.; Berry, D. H. *Adv. Organomet. Chem.* **1998**, *43*, 197, and references therein. (c) Speier, J. L. *Adv. Organomet. Chem.* **1979**, *17*, 407. (d) Hiyama, T.; Kusumoto, T. In *Comprehensive Organic Synthesis*; Trost, B. M., Fleming, I., Eds.; Pergamon Press: Oxford, 1991; Vol. 8, p 763. (e) Marciniec, B.; Gulinsky, J.; Urbaniak, W.; Kornetka, Z. W. *Comprehensive Handbook on Hydrosilylation*; Marciniec, B., Eds.; Pergamon: Oxford, U.K., 1992. (f) Molander, G. A.; Nichols, P. J. *J. Am. Chem. Soc.* **1995**, *117*, 4415. (g) Molander, G. H.; Nichols, P. J. *J. Org. Chem.* **1998**, *63*, 2292.

(27) (a) Chalk, A. J.; Harrod, J. F. *J. Am. Chem. Soc.* **1965**, *87*, 16. (b) Harrod, J. F.; Chalk, A. J. *J. Am. Chem. Soc.* **1965**, *87*, 1133. (c) Tanke, R. S.; Crabtree, R. H. *Organometallics* **1991**, *10*, 415. (d) Takeuchi, R.; Yasue, H. *Organometallics* **1996**, *15*, 2098. (e) Christ, M. L.; Sabo-Etienne, S.; Chaudert, B. *Organometallics* **1995**, *14*, 1082. Three main modified Chalk–Harrod mechanism have been postulated: (f) Seitz, F.; Wrighton, M. S. *Angew. Chem., Int. Ed. Engl.* **1988**, *27*, 289. (g) Duckett, S. B.; Perutz, R. N. *Organometallics* **1992**, *11*, 90. (h) Randolph, C. L.; Wrighton, M. S. *J. Am. Chem. Soc.* **1986**, *108*, 3366. (i) Ruiz, J.; Bentz, P. O.; Mann, B. E.; Spencer, C. M.; Taylor, B. F.; Maitlis, P. M. *J. Chem. Soc., Dalton Trans.* **1987**, 2709. (j) Brookhart, M.; Grant, B. E. *J. Am. Chem. Soc.* **1993**, *115*, 2151. (k) Bode, B. M.; Day, P. N.; Gordon, M. S. *J. Am. Chem. Soc.* **1998**, *120*, 1552. (l) Sakaki, S.; Mizoe, N.; Sugimoto, M. *Organometallics* **1998**, *17*, 2510. (m) Sakaki, S.; Ogawa, M.; Musashi, Y.; Arai, T. *J. Am. Chem. Soc.* **1994**, *116*, 7258.

(28) (a) Eisen, M. S. In *The Chemistry of Organosilicon Compounds*; Apeloig, Y., Rappoport, Z., Eds.; John Wiley: Chichester, Vol. 2, Part 3, 1998; Chapter 35, pp 2038–2122. (b) Eisen, M. S. *Rev. Inorg. Chem.* **1997**, *17*, 25. (c) Radu, N. S.; Engeler, M. P.; Gerlach, C. P.; Tilley, T. D.; Rheingold, A. L. *J. Am. Chem. Soc.* **1995**, *117*, 3621.

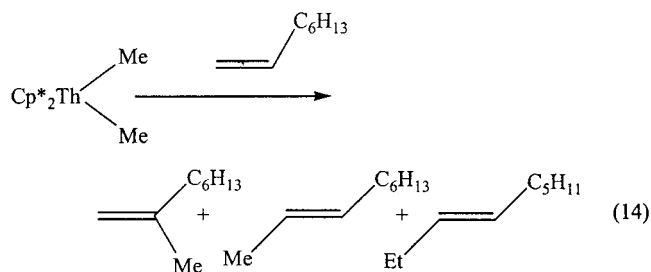
In all reactions we have found that with each one of the organoactinide complexes, $\text{Me}_2\text{SiCp}''_2\text{Th}^n\text{Bu}_2$ and Cp^*ThMe_2 , stoichiometric amounts of PhSiH_2Bu and PhSiH_2Me are obtained, respectively. This result corroborates with a rapid metathesis reaction between the precatalysts and the silane forming the corresponding hydride complexes as the first step in the reaction. The presence of the two major products (hydrosilylation and hydrogenation) indicates the existence of two parallel catalytic pathways. The formation of the hydrogenation products requires considering the possibility that the intermediates' Th–Si/Th–H bonds are formed (eq 13). Thus, the production of alkanes might be considered, to some extent, as indirect evidence of the existence of complexes containing a Th–Si bond. Protonolysis of a Th–carbyl by the silane will yield the Th–Si bond and the hydrogenation product, whereas metathesis of the Th–carbyl by the silane will produce the hydrosilylated compound regenerating the hydride complex.



Interestingly, by performing the reaction at higher temperatures, larger turnover frequencies are obtained, with a larger effect for the bridged unsaturated complex $\text{Me}_2\text{SiCp}''_2\text{Th}^n\text{Bu}_2$ than for the isolobal Cp^*ThMe_2 . Regarding the regiochemistry of each of the complexes, at different temperatures, no diverse major effects are observed. This result corroborates with two parallel pathways, plausibly interrelated, as exhibited by the consistent similar ratios among the products, which is preserved at the different conditions (compare entries 1–3 and 2–4 in Table 5).

Since another theoretical possibility to obtain a hydrogenation product from a Th–alkyl complex is conceivable by cutting the alkyl chain with an additional alkene, forming a transient vinyl complex, we have decided to study this possibility by performing the reaction between the Cp^*ThMe_2 and an excess of 1-octene. Although no hydrogenation products were observed, ruling out the protonolysis by an alkene, there is a stoichiometric reaction allowing the production of 2-methyl-1-octene, 2-nonene, and 3-nonene in almost equal amounts and an additional slow catalytic isomerization of the starting 1-octene to *E*-4-octene (3.8%), *E*-3-octene (39.4%), *E*-2-octene (13.0%), and *Z*-2-octene (41.8%). The characterization of all the isomers has been performed by GC and GC/MS retention times and by comparison with results obtained in similar isomerization with early-transition complexes (eq 14).⁹

This result clearly indicates that the Th–Me bond is able to insert into an alkene moiety forming a Th–alkyl complex, which β -hydrogen eliminates to the corresponding metal–hydride (Th–H) and equimolar amounts of all possible isomeric nonenes. The hydride will continue, under a similar mechanistic pathway, the isomerization of 1-octene. The same reaction under



identical conditions but with 2-octene shows that the reaction is much slower and different product ratios are obtained (*E*-3-octene (11.2%), *E*-2-octene (82.2%), and *Z*-2-octene (6.6%)). This result indicates that the reaction 1-octene \rightarrow 2-octene is not in equilibrium, because 1-octene was not obtained (trace amounts were also not formed).

Extremely important was to study the resting state of the organoactinide moiety in this reaction in view of the fact that only two complexes with either a thorium hydride (Th–H) or a thorium–alkyl (Th–R) are expected. Thus, we have performed the isomerization reaction until full conversion of 1-octene (>98%) was observed (140 h). The high-vacuum transfer of all the volatile organic products (10^{-6} mmHg) was performed, and solvent was reintroduced. The ratio between the products, which remained in the reaction mixture, was measured by GC chromatography (Figure 6a), showing almost full disappearance of 1-octene.

Quenching of the reaction mixture with the organometallic complexes present in the solution with a slight excess of D_2O at low temperatures, allowing the mixture to warm to room temperature, and GC and GC/MS chromatography of an aliquot of this solution shows the presence of a monodeuterated 1-*d*-octane, indicating that a Th–alkyl moiety is the resting organoactinide. This result proves that the insertion of an alkene with an organoactinide hydride is an extremely fast process.^{24,29} The most astonishing result was the GC chromatograph after the D_2O quenching, showing equimolar amounts of 1-octene, as compared with the starting amount of the metal complex (Figure 6b) (measured by the integration as compared with a calibration curve of pure 1-hexene). This result strongly indicates that a π -alkene thorium–alkyl complex is the most plausible resting catalytic state of the organoactinide complex under this reaction conditions. The addition of D_2O liberates the alkene and the alkane from the metal to the reaction mixture.

Kinetic Studies of the Hydrosilylation of Alkenes with PhSiH_3 . Kinetic measurements on the hydrosilylation of a \sim 100-fold excess of allylbenzene with PhSiH_3 catalyzed by Cp^*ThMe_2 were performed by in-situ ^1H NMR spectroscopy. The reaction was monitored with constant substrate concentrations until complete silane consumption. The disappearance of the silane hydride SiH_3 ($\delta = 4.26$ ppm) and the appearance of the triplet of $\text{C}_6\text{H}_5\text{CH}_2\text{CH}_2\text{SiH}_2\text{Ph}$ ($\delta = 4.51$ ppm) ^1H resonances were normalized. The turnover frequency of the reaction was calculated from the slope of the kinetic plots of substrate-to-catalyst ratio vs time. When the

(29) Lin, Z.; Marks, T. J. *J. Am. Chem. Soc.* **1990**, *112*, 5515, and references therein.

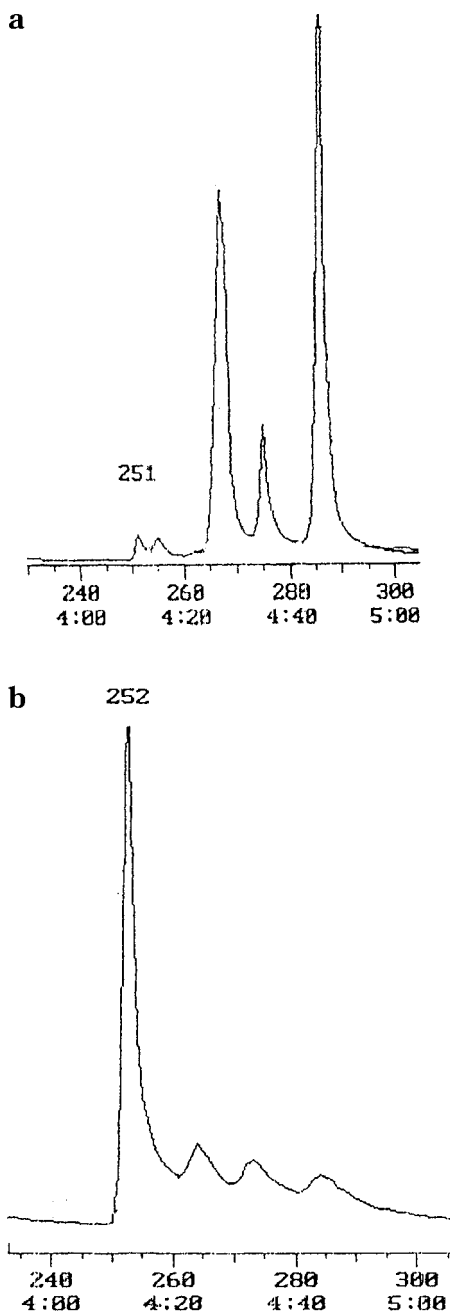


Figure 6. GC chromatograph of the reaction mixture of the isomerization of 1-octene. After the reaction is completed (**6a**), after quenching with D₂O (**6b**). The order of appearance of the alkenes in **6a** = 1-octene (position marked as 251) (2.0%), *E*-4-octene (3.8%), *E*-3-octene (39.4%), and *E*-2-octene (13.0%), and *Z*-2-octene (41.8%). In **6b**, 1-octene appears at position 252.

initial concentration of the alkene and the silane remain constant and the concentration of the catalytic precursor is varied over a ~13-fold concentration range, a plot of the reaction rate vs precatalyst concentration indicates that the reaction is first-order dependent on precatalyst.^{23a} When the concentration of the alkene and the catalyst are held constant and the concentration of the silane is changed over a ~10-fold concentration range, a plot of the reaction rate vs precatalyst concentration indicates that the reaction is first-order dependent on silane.^{23a} When the concentration of the silane and

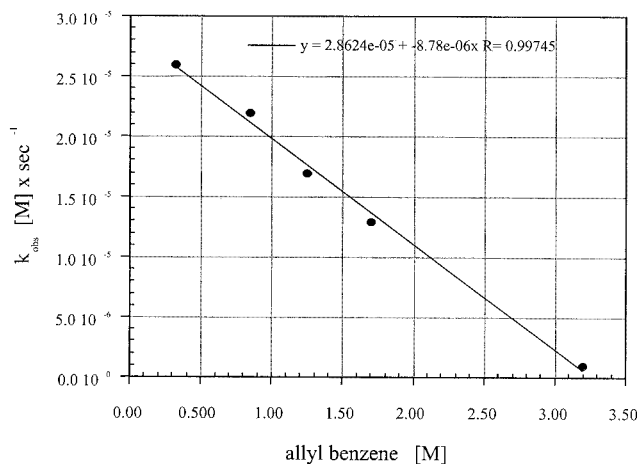


Figure 7. Determination of the reaction order in alkene concentration for the hydrosilylation of allyl benzene with PhSiH₃ mediated by Me₂SiCp*₂ThⁿBu₂ as the precatalyst in benzene-*d*₆ at 20 °C. The line represents the least-squares fit to the data points.

catalyst are kept constant and the alkene concentration is changed over a 10-fold concentration range (Figure 7), a plot of the reaction rate vs alkene concentration exhibits an inverse proportionality, indicating that the reaction is inverse first-order dependent on alkene. The inverse proportionality as described for alkynes is coherent with a rapid equilibrium prior to the rate-determining step, steering an intermediate out of the catalytic cycle. Thus, the rate law for the hydrosilylation of alkenes with PhSiH₃ promoted by Cp*₂ThMe₂ can be expressed as presented in eq 15.

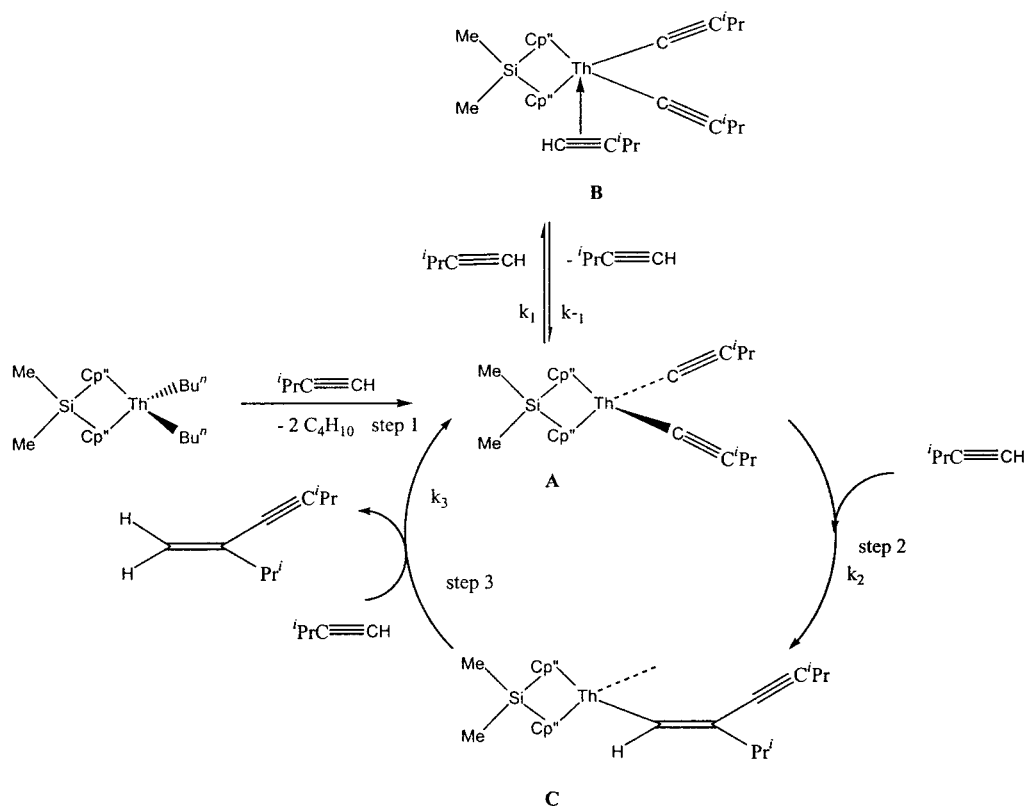
$$v = k[\text{Cp}^*_2\text{ThMe}_2][\text{silane}]^1[\text{alkene}]^{-1} \quad (15)$$

The derived E_a , ΔH^\ddagger , and ΔS^\ddagger parameter values (error values are in parentheses) from an Arrhenius and a thermal Eyring analysis are 11.0(4) and 10.3(4) kcal mol⁻¹ and -45 eu, respectively.^{23a}

Discussion

The discussion of the results will be presented by starting with the scope for the dimerization of terminal alkynes promoted by the bridged organothorium complex, followed by the hydrosilylation of alkynes and alkenes with PhSiH₃, the formation of a key intermediate in the D₂O quenching experiments reaction between an organoactinide and an olefin in the absence of a silane, and the mechanistic implications in each catalytic process.

Catalytic Dimerization of Terminal Alkynes: Reaction Scope and Mechanism. The catalytic results for the selective dimerization of terminal alkynes promoted by Me₂SiCp*₂ThⁿBu₂ rapidly produce the geminal olefins with high regioselectivity, in addition to small amounts of the corresponding alkyne trimer, which were observed only for some alkynes. A substantial range of substrates can be selectively dimerized including bulky, nonbulky, or alkyne containing an olefin substituent. Interestingly, for (TMS)C=CH no dimerization or oligomerization was obtained, although butane was evolved. It seems that the energy of activation for an alkyne metathesis with the moiety Th-C=

Scheme 2. Plausible Mechanism for the Dimerization of Terminal Alkynes Promoted by $\text{Me}_2\text{SiCp}''_2\text{Th}^n\text{Bu}_2$ 

C(TMS) obtained from the coordinative unsaturated complex $\text{Me}_2\text{SiCp}''_2\text{Th}^n\text{Bu}_2$ is by far higher ($> \sim 14.8$ kcal/mol) than the similar metathesis from the corresponding $\text{Cp}''_2\text{ThMe}_2$, where both geminal dimer and the head-to-tail-to-head trimer were observed.^{22,30} Since the stereochemical approach of an alkyne to the organometallic moiety is via a side approach, it is reasonable to consider that the insertion of alkyne will be encountered always facing its substituent away from the metal center, allowing the highly regioselective production of the geminal dimers. The methyl groups of the cyclopentadienyl spectator ligation encumber the disposition of the alkyne substituent facing the metal center.

A plausible mechanism for the selective dimerization of $i\text{PrC}\equiv\text{CH}$ promoted by $\text{Me}_2\text{SiCp}''_2\text{Th}^n\text{Bu}_2$ is presented in Scheme 2. The mechanism consists of a sequence of entrenched straightforward reactions such as terminal alkyne insertion into a metal–carbon σ -bond and σ -bond metathesis. The initial step in the catalytic cycle is the alkyne C–H activation by the complex $\text{Me}_2\text{SiCp}''_2\text{Th}^n\text{Bu}_2$ and the formation of the bisacetylide complex **A** together with butane (step 1). Complex **A** either may be in equilibrium with an alkyne forming the proposed π -alkyne acetylide complex **B**, which drives the active species out of the catalytic cycle (inverse rate dependence), or undergoes with another alkyne a head-to-tail insertion into the thorium–carbon σ -bond, yielding the substituted alkenyl complex **C** (step 2).³¹ This complex undergoes a σ -bond protonolysis with an additional

alkyne (step 3), leading to the corresponding dimer and regenerating the active acetylide complex **A**.³²

The alkyne π -complex **B** is proposed on the basis of similar kinetic alkyne behavior observed for the cationic coordinative unsaturated uranium complex $[(\text{Et}_2\text{N})_3\text{U}][\text{BPh}_4]$, for which a similar complex **B** has been trapped, and the structure was determined spectroscopically.²⁴ The turnover-limiting step for the catalytic dimerization is the insertion of the alkyne into the thorium–acetylide complex **A** (step 2). This result suggests that the σ -bond metathesis between the complex $\text{Me}_2\text{SiCp}''_2\text{Th}^n\text{Bu}_2$ and the alkyne (step 1) and the protonolysis of **C** by the alkyne acidic proton are faster than the insertion of the alkyne into complex **A**. In addition, this result argues that trimers are only expected if a kinetic delay in the protonolysis is induced, corroborating our observations.³³ Thus, the derived rate law based on the mechanism proposed in Scheme 2 for the oligomerization of terminal alkynes promoted by the complex $\text{Me}_2\text{SiCp}''_2\text{Th}^n\text{Bu}_2$ is given by eq 16, fitting the kinetic performances of the alkyne and catalysts.³⁴

$$\nu = \frac{k_{-1}k_2[\text{cat}]}{k_1 + k_2 - \frac{k_2k_{-2}}{k_3[\text{alkyne}]}} \quad (16)$$

(31) In the proposed catalytic cycle, an intermediate (reactive isomer of **B**) could also appear between **A** and **C**, which is at a rapid steady state, before the insertion of the second alkyne.

(32) No Ellington oxidizing coupling products ($\text{RC}=\text{C}=\text{CR}$) were observed.

(33) If the protonolysis of the alkyne is the rate-limiting step, a large number of oligomers are expected.

(34) For a full derivation of the kinetic rate expression based on the mechanism as presented in Scheme 2, see ref 28b.

(30) The energy of activation value is estimated from the known value of 11.8 kcal·mol⁻¹ for the metathesis of an alkyne into a thorium–acetylide bond, in addition to 3 kcal·mol, since no product was found.²⁶ The value of 3 kcal·mol is assigned from the chemoselectivity value of >99% yield from $\Delta G^\ddagger = -RT \ln(k)$.

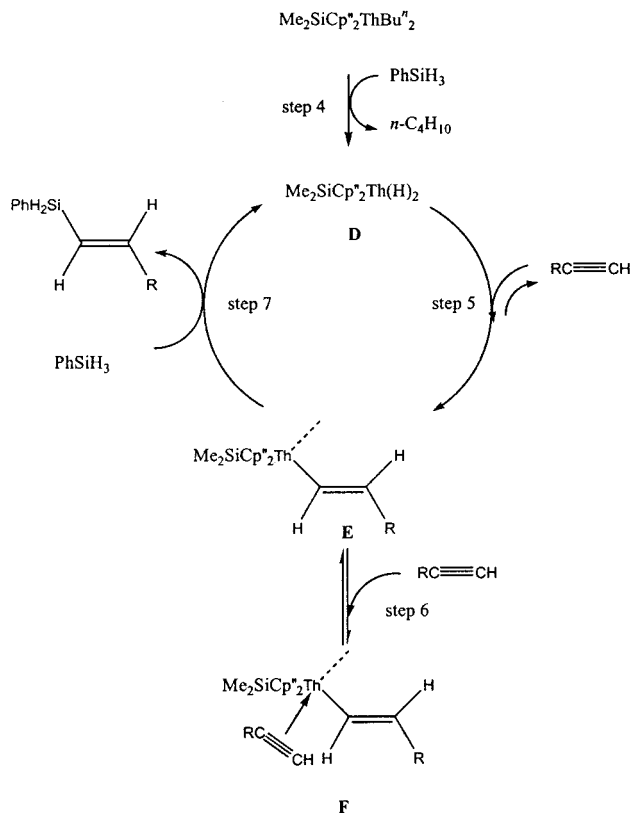
The activation parameters of the organothorium-catalyzed dimerization are characterized by a rather small enthalpy of activation (11.7(3) kcal mol⁻¹) and a large negative entropy of activation (-22.6(6) eu; $\Delta G^\ddagger_{298} = 18.4(6)$ kcal mol⁻¹). These parameters suggest a highly ordered transition state with considerable bond making to compensate the bond breaking. Interestingly, organoactinide-centered hydrogenolysis processes with Cp^{*}₂ThMe₂, which proceed via a four-centered transition state, exhibit similar activation parameters and smaller entropic values ($\Delta H^\ddagger = 9(2)$ kcal mol⁻¹, $\Delta S^\ddagger = -45(5)$ eu), whereas for the organouranium cationic complex [(Et₂N)₃U][BPh₄] similar enthalpy values are observed, although a higher entropic value is obtained due to its larger coordinative unsaturation as compared to the bridged organoactinide ($\Delta H^\ddagger = 15.6(3)$ kcal mol⁻¹, $\Delta S^\ddagger = -11.4(6)$ eu). Thus, it seems that the entropy measured for a concerted four-centered transition state can be used as a qualitative measure of the coordinative unsaturation for an organoactinide complex in the rate-determining step (the higher the value, the more unsaturated) following the order [(Et₂N)₃U][BPh₄] > Me₂SiCp^{*}₂ThⁿBu₂ > Cp^{*}₂ThMe₂.

Catalytic Hydrosilylation of Terminal Alkynes: Scope and Mechanism. The catalytic results for the hydrosilylation of terminal alkynes with PhSiH₃ promoted by Me₂SiCp^{*}₂ThⁿBu₂ produce regio- and chemoselectively the *trans*-hydrosilylated vinylsilane without any other byproducts. This result demonstrates the ability to tailor the hydrosilylation reaction catalyzed by organoactinides by modulating the spectator ancillary ligation.⁶ Moreover, the absence of silylalkynes, the dehydrogenative silane coupling products, or any other geometrical isomer of the vinylsilane strongly indicates that the Th-H pathway is the major operative route in the hydrosilylation reaction. The formation of a Th-Si bond should produce the *cis*- or the *geminal*-hydrosilylated products and possible small amounts of alkenes, all of them absent under the reaction conditions.

Thus a plausible mechanism for the hydrosilylation of terminal alkynes toward *trans*-vinylsilanes is presented in Scheme 3.

The mechanism presented in Scheme 3 consists of a sequence of elementary reactions such as insertion of an alkyne into a metal-hydride σ -bond and σ -bond metathesis by a silane. The precatalyst Me₂SiCp^{*}₂ThⁿBu₂ in the presence of silane and alkyne is converted into the hydride complex **D** (step 4), as observed by the stoichiometric formation of *n*-BuSiH₂Ph (characterized by GC and GC/MS chromatography).³⁵ Rapid insertion of an alkyne into complex **D** allows the formation of the vinylic complex **E** (step 5). For organoactinides, this process has been found to be in rapid equilibrium.²⁹ Complex **E** either may be in *rapid equilibrium* with the proposed π -complex **F** (step 6), responsible for the inverse order in alkyne, or undergoes a σ -bond metathesis with PhSiH₃, as the rate-determining step (step 7), producing selectively the *trans*-hydrosilylated vinyl product and regenerating complex **D**. It is important to point out that no geometrical isomers or different products were observed by adding an excess of PhSiH₃

Scheme 3. Plausible Mechanism for the Hydrosilylation of Terminal Alkynes with PhSiH₃ Promoted by Me₂SiCp^{*}₂ThⁿBu₂^a



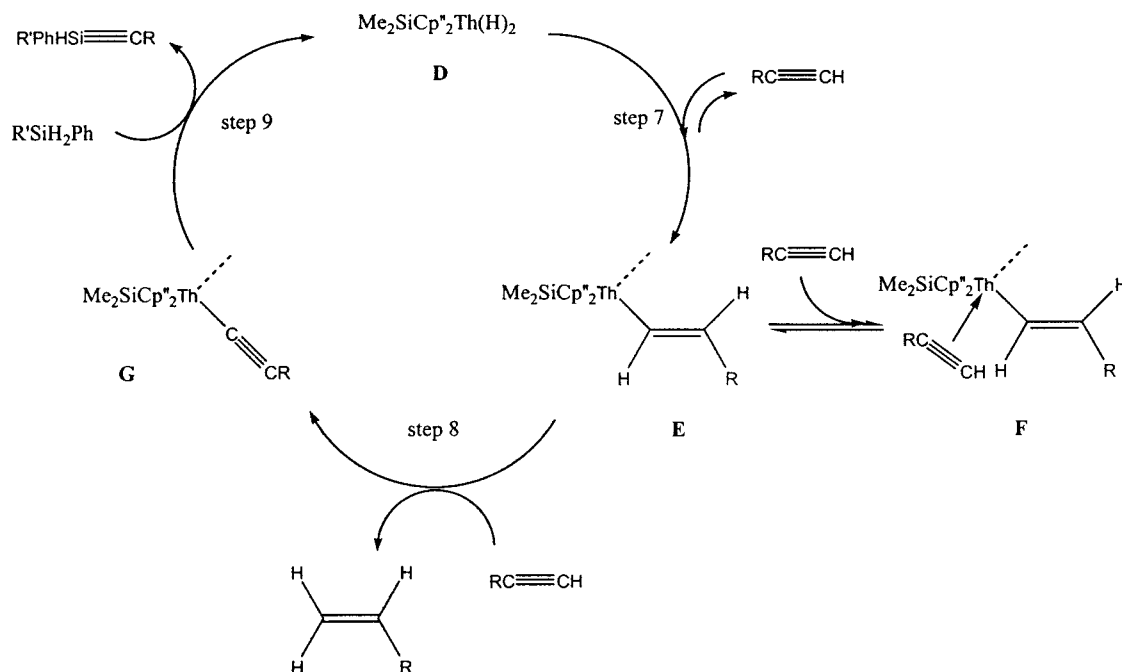
^a Only one of the equatorial ligations at the metal center is shown for clarity.

to any of the vinylsilane products. This result indicates that neither the hydride complex **D** nor the alkenyl complex **E** is the resting catalytic state for this process under these conditions (products from the dehydrogenative coupling of the silane are expected)²⁴ and points toward complex **F** as the resting state for this organoactinide. However, the subsequent addition of a second equivalent of an alkyne to the reaction mixture allows the formation of the corresponding alkene, and the silylalkyne resulted from the dehydrogenative coupling of the alkyne with the *trans*-vinylsilane. The plausible formation of these two compounds is shown in Scheme 4. In this cycle, complex **E** reacts, in the absence of a primary silane, with another alkyne (step 8), affording the corresponding alkene and the acetylide complex **G**. Complex **G** undergoes a σ -bond metathesis with the Si-H bond of the vinylsilane (step 9), forming the dehydrogenative coupling product and regenerating the hydride complex **D**. These processes, as presented in Scheme 4, are similar to those found in the catalytic hydrosilylation of terminal alkynes promoted by precatalyst Cp^{*}₂ThMe₂.⁶ It is noteworthy to point out that the yield of the alkene is much lower than that of the silylalkyne product.

This result suggests that an additional equilibrium reaction is operative, responsible for the transformation of complex **D** into the acetylide complex **G**, allowing the formation of the silylalkyne without forming the alkene (eq 17). Similar equilibrium has been established in the hydrosilylation of terminal alkynes with PhSiH₃ cata-

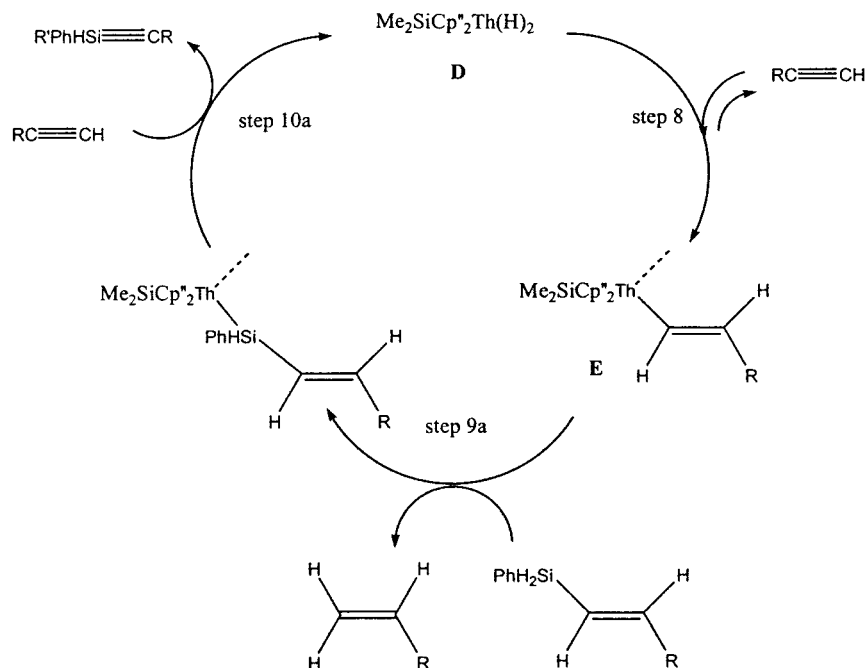
(35) Attempts to trap and characterize the resulting organometallic hydride were unsuccessful possibly due to different isomeric structures (dimer, trimers, etc). For Cp^{*}₂ThH₂ this complex exists as a dimer, see ref 3c.

Scheme 4. Plausible Mechanism for the Formation of Alkene and Silylalkyne in the Presence of Vinylsilanes and Terminal Alkynes Promoted by $\text{Me}_2\text{SiCp}''_2\text{Th}^n\text{Bu}_2^a$



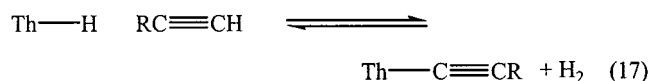
^a Only one of the equatorial ligations at the metal center is shown for clarity.

Scheme 5. Theoretical Mechanism for the Formation of Alkene and Silylalkyne in the Presence of Vinylsilanes and Terminal Alkynes Promoted by $\text{Me}_2\text{SiCp}''_2\text{Th}^n\text{Bu}_2^a$



^a Only one of the equatorial ligations at the metal center is shown for clarity.

lyzed by the nonbridged organoactinides.⁶ In addition this result argues against the theoretical silane pathway (steps 9a and 10a in Scheme 5) given that equimolar amounts of each silylalkynes and alkene are expected.



The activation energy parameters for the hydrosilylation of $^i\text{PrC}\equiv\text{CH}$ with PhSiH_3 promoted by $\text{Me}_2\text{SiCp}''_2$ -

Th^nBu_2 are characterized by an enthalpy of activation similar to that for the dimerization of alkynes ($\Delta H^\ddagger = 10.07(5) \text{ kcal mol}^{-1}$, $E_a = 9.47(5) \text{ kcal mol}^{-1}$) and a large negative entropy of activation ($\Delta S^\ddagger = -22.06(5) \text{ eu}$, $\Delta G^\ddagger = 16.6(5) \text{ kcal mol}^{-1}$ at 298 K). These parameters suggest again as shown before a highly ordered transition state with considerable bond-making to compensate for bond-breaking. Thus, the process proceeds with a high degree of entropic reorganization on approaching the transition state. The low ΔG^\ddagger of activation

indicates that the σ -bond metathesis of the alkenyl complex by PhSiH_3 , which is the rate-determining step, is faster as compared to the insertion of an alkyne into the bis(acetylide) complex ($\Delta G^\ddagger = 18.4$ (6) kcal mol⁻¹), which will produce alkyne oligomers.

The ratio between the primary silane and the alkyne seems to govern the kinetics toward the different products. Thus, when the $\text{PhSiH}_3:\text{PrC}\equiv\text{CH}$ ratio is equimolar, the *trans*-hydrosilylation product is the only one indicating that the metathesis route (step 7 in Scheme 3) is faster than protonolysis by the alkyne (step 8 in Scheme 4). An increase in the alkyne concentration routes the reaction, in the absence of primary silane, toward the alkene and the silylalkyne, the dehydrogenative coupling product. Interestingly, the absence of the expected alkyne oligomerization products under this PhSiH_3 -starving conditions suggests that the metathesis reaction of the bis(acetylide) complex with the vinylsilane product (step 9 Scheme 4) is much faster than that of the insertion of an alkyne into the bis(acetylide) complex **G** (step 2 in Figure 1). The low reactivity of the secondary silanes and their intrinsic inability toward the σ -bond metathesis route to produce the corresponding vinylsilane seems to be responsible for allowing the production of alkene and the bis(acetylide) complex, which may react slowly with the silane producing the silylalkyne and the corresponding hydride.

Regarding the rates, the present hydrosilylation process exhibits larger turnover frequencies as compared to $\text{Cp}^*_2\text{YCH}_3\cdot\text{THF}$ or other lanthanide complexes.^{7,36} The yttrium complex is able to induce the hydrosilylation reaction of internal alkynes preferentially toward the *E*-isomer, although in some case the *Z*-isomer is found in similar quantities. Mechanistically, the active species for the yttrium hydrosilylation of internal alkynes is proposed to be the corresponding hydride.³⁷ It is well known that the hydrosilylation of alkynes is induced either by radical initiators³⁸ or by transition metal catalysts.^{26,27,39} The radical-induced procedure often provides a mixture of *trans*- and *cis*-hydrosilylation products, although the transition metal catalyzed reaction proceeds with high stereoselectivity via a *cis*-hydrosilylation pathway; it usually produces a mixture of two regioisomers (terminal and internal adducts). Thus, this organoactinide process seems to contain a unique chemical environment, allowing the production of the *trans*-vinylsilane complementing the chemistry of other transition metal complexes.

Catalytic Hydrosilylation of Alkenes Catalyzed by $\text{Me}_2\text{SiCp}''_2\text{Th}^n\text{Bu}_2$ and $\text{Cp}^*_2\text{ThMe}_2$. The hydrosilylation of alkenes with PhSiH_3 promoted by $\text{Me}_2\text{SiCp}''_2\text{Th}^n\text{Bu}_2$ and $\text{Cp}^*_2\text{ThMe}_2$ produces the formation of

1-silylalkanes with comparable amounts of the corresponding alkanes (besides styrene both 1,2- and 2,1-hydrosilylated adducts were obtained). Moreover, the fast (even at low temperatures) production of stoichiometric amounts of PhSiH_2R ($\text{R} = \text{Me}$ or Bu) for $\text{Cp}^*_2\text{ThMe}_2$ and $\text{Me}_2\text{SiCp}''_2\text{Th}^n\text{Bu}_2$, respectively, indicates that the first step in the catalytic cycle is the fast formation of the corresponding Th–H bonds. Furthermore, small amounts of Ph_2SiH_2 and traces of oligomeric silane products obtained from the dehydrogenative coupling of PhSiH_3 comprise the additional compounds observed in the hydrosilylation reactions of *all* alkenes for *both* organoactinides regardless of the temperature at which the reaction was performed. A comparison between the products' distribution, using both organoactinides in all the alkene reactions, reveals that no special effect is present by increasing the coordinative unsaturation of the organothorium complex. Moreover, the concomitant presence of the two products suggests the existence of two parallel interconnecting competing pathways. Performing the reaction at a higher temperature (78 °C), as compared to room temperature, illustrates that almost no variation in the product yields is noticed (both processes are conducted equally at both temperatures). Nevertheless, it is worth pointing that there is a significant difference in the turnover frequencies between the hydrosilylation catalyzed by $\text{Cp}^*_2\text{ThMe}_2$ or $\text{Me}_2\text{SiCp}''_2\text{Th}^n\text{Bu}_2$. For the former complex an increase in the reaction temperature corresponded to a 2-fold increase in the kinetic rate, whereas for the latter complex an order of magnitude augmentation in the rate of the reaction was observed.

The formation of the alkane requires considering the intermediate Th–H/Th–Si moieties. The only evidence so far for the existence of a Th–Si bond has been the formation of a metalloxy ketene via the double insertion of carbon monoxide into a Th–Si bond.^{28a,c} The kinetic rate equations for the organoactinide-catalyzed hydrosilylation of terminal alkynes (eq 10) and alkenes (eq 15) seem to be practically related to the production of the byproducts in the latter catalytic process. Hence, a plausible mechanism for the hydrosilylation of alkenes promoted by organoactinides consistent with the formation of all products is described in Scheme 6.

The mechanism consists of simple reactions, which have already been observed in other organoactinide-promoted catalytic processes. The first step in the mechanism is the reaction of the precatalyst $\text{Cp}^*_2\text{ThMe}_2$ with PhSiH_3 yielding the hydride complex **H** and PhSiH_2Me . Complex **H** reacts with an alkene, producing the alkyl complex **I** (step 11), which may undergo three parallel pathways. The first pathway is a reaction with an alkene, producing a π -alkene complex (**J**), driving complex **I** out of the catalytic cycle (step 12), and is responsible for the inverse order in alkene. The second and third route are either a metathesis or a protonolysis between the Th–carbonyl fragment with the Si–H moiety yielding in the former case the substituted silane and regenerating complex **H** (step 13) or in the latter process yielding the Th–SiH₂Ph complex and the alkane (step 14).

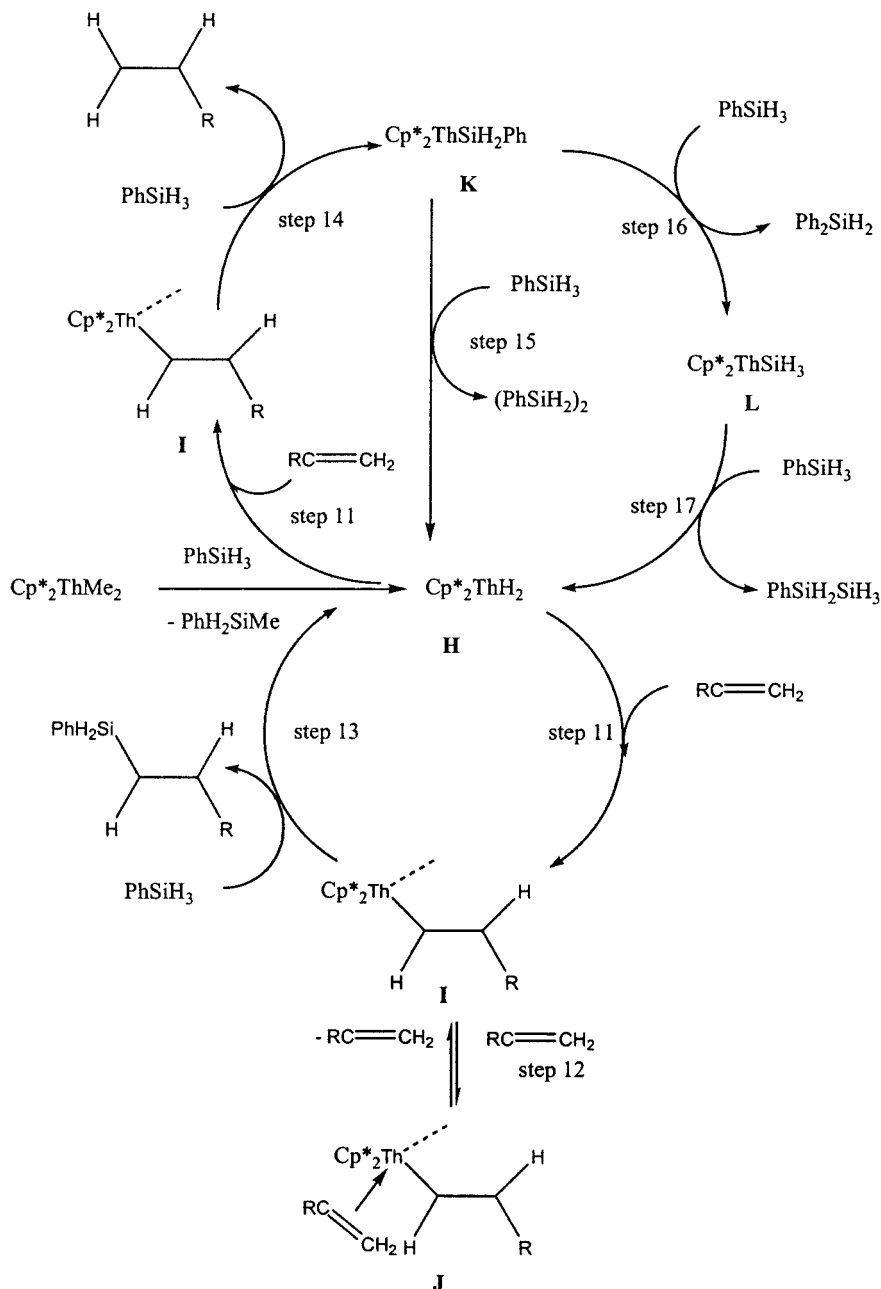
Similar energy of activations for those two processes, which differ only in the disposition of the silane with

(36) Schumann, H.; Keitsch, M. R.; Demtschuk, J.; Molander, G. A. *J. Organomet. Chem.* **1999**, *582*, 70.

(37) Molander, G. A.; Knight, E. E. *J. Org. Chem.* **1998**, *63*, 7009.

(38) (a) Selin, T. J.; West, R. *J. Am. Chem. Soc.* **1962**, *84*, 1860. (b) Benkeser, R. A.; Burrous, M. L.; Nelson, L. E.; Swisher, J. V. *J. Chem. Soc.* **1961**, *83*, 4385.

(39) Transition metal complexes derived from Pt, Ir, Pd, Rh, Ru, Ni, Co, Fe, Re, and Mn metals have been used for hydrosilylation, see: (a) Hiyama, T.; Kusumoto, T. In *Comprehensive Organic Synthesis*; Trost, B. M., Fleming, I., Eds.; Pergamon Press: Oxford, 1991; Vol. 8, p 763. (b) Weber, W. P. *Silicon Reagents for Organic Synthesis*; Springer-Verlag: Berlin, 1983. (c) For aluminum compounds see: Asao, N.; Sudo, T.; Yamamoto, Y. *J. Org. Chem.* **1996**, *61*, 7654. (d) Sudo, T.; Asao, N.; Gevorgyan, V.; Yamamoto, Y. *J. Org. Chem.* **1999**, *64*, 2494.

Scheme 6. Plausible Mechanism for the Hydrosilylation of Alkenes and PhSiH₃ Promoted by Cp*₂ThMe₂ or Me₂SiCp*₂ThⁿBu₂^a


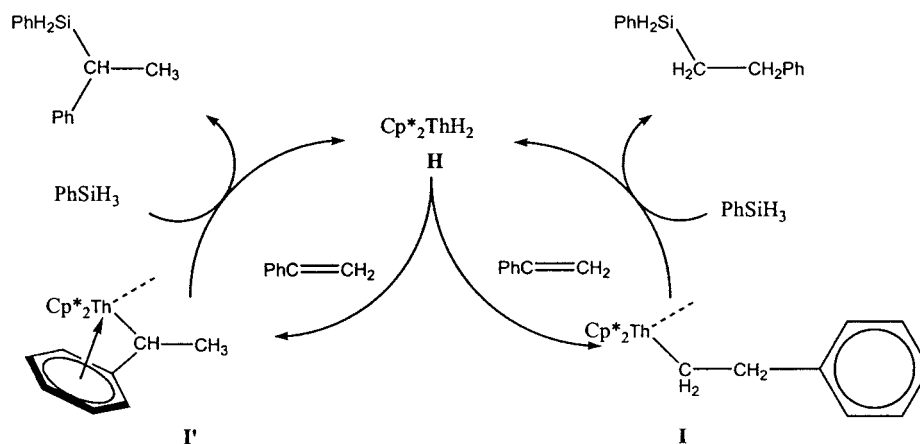
^aThe scheme depicts the mechanism for the former complex. Only one of the equatorial ligands at the metal center is shown for clarity.

respect to the thorium carbonyl complex, indicates the lack of discrimination between these two pathways, allowing similar yields of the two products at various temperatures. The Th–SiH₂Ph (**K**) bond can be activated by two different methods. The metathesis reaction with the Si–H bond in PhSiH₃ produces the dehydrogenative dimer and the hydride **H** (step 15), whereas the reaction with the Si–Ph bond will allow the formation of the Ph₂SiH₂ and a complex containing the Th–SiH₃ (**L**) moiety (step 16), which will react rapidly with an additional silane, yielding oligomeric dehydrogenative coupling of silanes (step 17). This latter Ph₂SiH₂ has been trapped and fully characterized by its comparison to a commercially available sample. The presence of trace amounts of various oligomeric silanes beyond the dimer-

ic (PhSiH₂)₂ impeded their complete separation and full characterization.

In the hydrosilylation of styrene besides the hydrogenation ethylbenzene, the dehydrogenative dimer [PhH₂Si]₂, and the 1,2-addition hydrosilylation alkane, the 2,1-addition hydrosilylation product was also observed. For Cp*₂ThMe₂ only ~6% of this second isomer was obtained, whereas for the coordinative unsaturated Me₂SiCp*₂ThⁿBu₂ equimolar amounts of the hydrogenation or the 1,2-addition products were yielded. The formation of the second hydrosilylated isomer can be explained by the stereochemistry in the metathesis reaction of the styrene with the metal hydride complex (Scheme 7), which is plausibly stabilized by a π-arene interaction (**I**), as observed in the hydrosilylation of styrene by

Scheme 7. Plausible Mechanism for the Hydrosilylation of Styrene and PhSiH₃ Promoted by Cp*₂ThMe₂ or Me₂SiCp*₂ThⁿBu₂^a



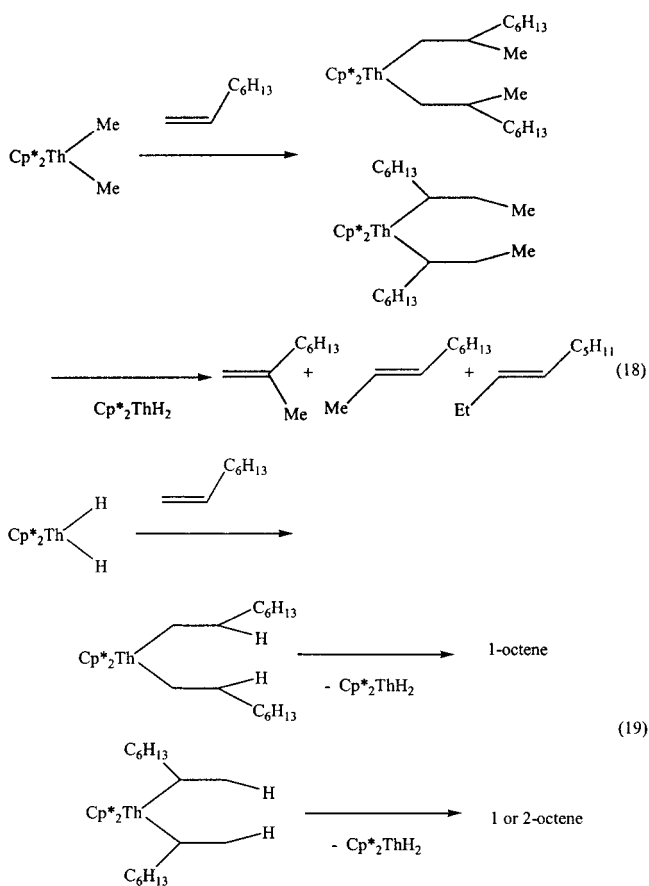
^a For the former complex, Scheme 7 is presented. Only one of the equatorial ligands at the metal center is shown for clarity.

lanthanide complexes.^{7a} Important to note is that the higher the coordinative unsaturation of a complex, the higher the π -arene stabilization, leading to higher yields of the 2,1-adduct. There is considerable precedent for such η^2 -benzylic structures in organo-f-element chemistry.^{4b,40} It is interesting to compare the results in the hydrosilylation of styrene with allylbenzene. For the latter substrate, both organoactinides produced exclusively the 1,2-adduct hydrosilylation alkane (**I**, Scheme 7). In allylbenzene the aromatic ring is disposed one methylene group farther away from the double bond that undergoes metathesis with the metal, indicating the strong effect of the acidity of the metal, tailoring the selectivity in the product formation.

For alkenes, the hydrosilylation reactions promoted by organolanthanides of the types Cp*₂LnR (Ln = Sm, La, Lu) or Me₂SiCp*₂SmR are much faster (by 1 order of magnitude) than those obtained with organoactinides. The major difference is found for linear α -alkenes, which lanthanides will hydrosilylate, forming both isomers, whereas actinides will exclusively yield the 1,2-adduct product. Mechanistically, the lanthanide hydrides have been proposed as the primordial pathway toward the hydrosilylated products.^{7a} Thus, organoactinides represent complementary catalysts to organolanthanide and other transition metal complexes for the regioselective hydrosilylation of α -olefins.

The most remarkable result was obtained from the reaction of the precatalyst Cp*₂ThMe₂ and 1-octene in the absence of the silane. The reaction was rather slow, and stoichiometric amounts of isomeric nonenes (2-methyloctane, 2-nonene, and 3-nonene) were observed. Those stoichiometric compounds and a Th–hydride complex result from the insertion of 1-octene into the starting Th–Me bond with subsequent β -hydrogen elimination (eq 18). The following reaction of 1-octene with the Th–H allows either the nonproductive reaction toward the Th–octyl complex, which upon β -hydrogen elimination yields back 1-octene, or the isomerization toward 2-, 3-, or 4-octene as observed for 1-octene (eq

19) and similarly discovered for early transition metal complexes.⁹



When the isomerization of 1-octene was completed quantitatively, GC chromatography of the reaction mixture left after evaporation of all volatiles (Figure 6a) shows that 1-octene is not present as a *free* organic molecule in the reaction mixture. D₂O quenching studies of the nonvolatile, remaining mixture followed by GC and GC/MS analysis of the reaction mixture indicate the presence of stoichiometric quantities of 1-*d*-octane and *surprisingly* 1-octene (Figure 6b). Hence, in the absence of silanes it seems very likely that a π -alkene thorium–alkyl complex **J** consists of the resting state

(40) (a) Eisen, M. S.; Marks, T. J. *Organometallics* **1992**, *11*, 3939. (b) Eisen, M. S.; Marks, T. J. *J. Mol. Catal.* **1994**, *86*, 23. (c) Evans, W. J.; Ulibarri, T. A.; Ziller, J. W. *J. Am. Chem. Soc.* **1990**, *112*, 219. (d) Mintz, E. A.; Moloy, K. G.; Marks, T. J.; Day, V. W. *J. Am. Chem. Soc.* **1982**, *104*, 4692.

in the catalytic hydrosilylation of alkenes and probably similar structures involve the resting states in the other catalytic cycles, most likely responsible for the inverse order obtained in the kinetic studies.

Conclusions

This thorough study describes the catalytic activity of the bridge organothorium complex $\text{Me}_2\text{SiCp}''_2\text{Th}''\text{Bu}_2$ in the dimerization of terminal alkynes and in the hydrosilylation of terminal alkynes with PhSiH_3 with a comparison of the corresponding nonbridged complex $\text{Cp}^*_2\text{ThMe}_2$. In addition, the hydrosilylation of alkenes is presented for both organothorium complexes. In all three catalytic reactions a kinetic inverse order is obtained for the olefins/alkyne, indicating a possible π -olefin/alkyne complex. The reaction of $\text{Cp}^*_2\text{ThMe}_2$ with 1-octene produces the isomerization products in addition to isomeric nonenes. The D_2O quenching experiments corroborate with the formation of a π -olefin alkyl intermediate accountable for the inverse kinetic order. Opening the coordination sphere of the metal center by pulling back the cyclopentadienyl rings, using the bridging Me_2Si unit, allows faster and regioselective processes for the dimerization or the hydrosilylation of terminal alkynes. In the hydrosilylation of alkenes, opening the coordinative unsaturation of the complex allows only a rate improving. For the first two processes

the high regiochemistry is acquired by the selective hindrance of the equatorial plane by the methyl groups of the cyclopentadienyl rings, allowing the approach of the alkyne or the silane in a specific manner; in the latter process, a similar high regioselectivity is obtained regardless of the organoactinide used, although a lower chemoselectivity is obtained due to the associated hydrogenation products. The use of other *ansa*-organoactinides in similar processes is under investigation.

Acknowledgment. This research was supported by The Israel Science Foundation, administered by The Israel Academy of Sciences and Humanities under contract 83/01-1, by the E. and J. Bishop Research Fund, and by the Technion V.P.R. Fund, P. and E. Nathan Research Fund. M.S.E thanks the Humboldt Foundation for support during the preparation of the manuscript. A.K.D. thanks the Technion for a postdoctoral fellowship.

Supporting Information Available: Experimental details and characterization of compounds (**1**, **2**, **4**, **6**, **10**, **11**, **12**, **13**, **19**, **22**, and **23**), kinetic and thermodynamic plots for the dimerization of terminal alkynes and the hydrosilylation of terminal alkyne and alkenes, and X-ray tables for the complex $[\text{Me}_2\text{SiCp}''_2\text{Th}(\mu\text{-Cl}_4)\{\text{Li}(\text{DME})\}_2]$. This material is available free of charge via the Internet at <http://pubs.acs.org>.

OM010488S